Ore Geology Reviews 72 (2016) 86–113

Contents lists available at ScienceDirect

Ore Geology Reviews

journal homepage: www.elsevier.com/locate/oregeorev

Multicommodity mineral systems analysis highlighting mineral prospectivity in the Halls Creek Orogen

Sandra A. Occhipinti [a,*], Vaclav Metelka [a], Mark D. Lindsay [a], Julie A. Hollis [b], Alan R.A. Aitken [a], Ian M. Tyler [c], John M. Miller [a], T. Campbell McCuaig [a]

[a] Centre for Exploration Targeting, School of Earth and Environment, University of Western Australia, Crawley, Western Australia 6009, Australia
[b] Ministry of Mineral Resources, 3900 Nuuk, Greenland
[c] Geological Survey of Western Australia, Department of Minerals and Petroleum, East Perth, Western Australia 6004, Australia

ARTICLE INFO

Article history:
Received 20 February 2015
Received in revised form 3 July 2015
Accepted 6 July 2015
Available online 9 July 2015

Keywords:
Mineral systems
Hooper Orogeny
Halls Creek Orogeny
Halls Creek Orogen
Lamboo Complex
Deep crustal-scale structures

ABSTRACT

Understanding the regional context of mineral prospectivity is essential for opening areas to effective exploration. The Halls Creek Orogen in Western Australia, is one such region. Here we have completed a multicommodity mineral systems analysis, which we have used as a basis for the production of semi-automated prospectivity models. Known mineral occurrences or deposits formed over a period dominated by the compressional 1865–1850 Ma Hooper and 1835–1805 Ma Halls Creek orogenies, either followed, or preceded by periods of extension. Prospectivity models were built on knowledge-based fuzzy inference networks for seven commodity groups. The work has demonstrated a link between key model components and the propensity of disparate styles of mineral deposits to occur in this region, which has not been documented before. Different tectonic terranes defined as 'zones' in the Halls Creek Orogen are prospective for different commodity groups. A link between major crustal-scale faults or shear zones and the location of known ore deposits and occurrences in the area has been established. Many structures are either newly discovered, or their extension through the upper crust and down to the Moho has just been established. The lithospheric scale of these structurally weak zones would allow fluid migration from within, or below the lower crust. Of these structures, orogen perpendicular (northwest trending) and orogen oblique (north trending) faults are the most influential structures with respect to ore deposition, especially in regions where they intersect each other. The orogen-parallel structures were found to be less important. The crustal-scale architecture of the region and its link to known mineral occurrences suggests that the mineral prospectivity of the Halls Creek Orogen for commodities such as Ni, Cu, PGEs, Au, Pb, Zn and diamonds could be extended beyond known occurrences into the new zones delineated by the prospectivity analysis.

1. Introduction

The aim of this study was to systematically define mineral prospectivity at a regional-scale for the Halls Creek Orogen (Fig. 1). The region has exploration potential for several commodities; however, current public-domain knowledge of its prospectivity is extremely limited. This problem can be approached using a mineral systems analysis, in which ore deposits are understood to be small-scale expressions of a range of earth processes that occur at different spatial and temporal scales (McCuaig and Hronsky, 2014). This approach can be applied to multiple commodities by the following.

- First analysing the tectonic framework of the region (Lindsay et al., 2015b, c);
- Determining the most likely periods of mineralisation of certain commodity groups;
- Delineating units considered to be fertile for certain commodity group, or proxies for fertility;
- Constructing a combined structural map from geophysical and geological datasets that inform ideas regarding fluid pathways and depositional trap sites for mineralisation (Lindsay et al., 2015b, c);
- Producing maps derived from Geological Survey of Western Australia (GSWA) datasets and geophysical analyses to generate a semi-automated prospectivity analysis.

In recent years there has been much emphasis placed on collating proxies for source, pathways and traps for the purpose of mineral systems analysis (Lindsay et al., 2015c; Joly et al., 2012). This has led to the use of geographic information system (GIS) based predictor maps as a method for delineating these proxies for disparate types of mineral systems. Such an approach has been variously discussed by Begg et al. (2009), Begg et al. (2010); McCuaig et al. (2010); and McCuaig and Hronsky (2014). However, for this analysis we used a more generic

* Corresponding author.

http://dx.doi.org/10.1016/j.oregeorev.2015.07.003
0169-1368/

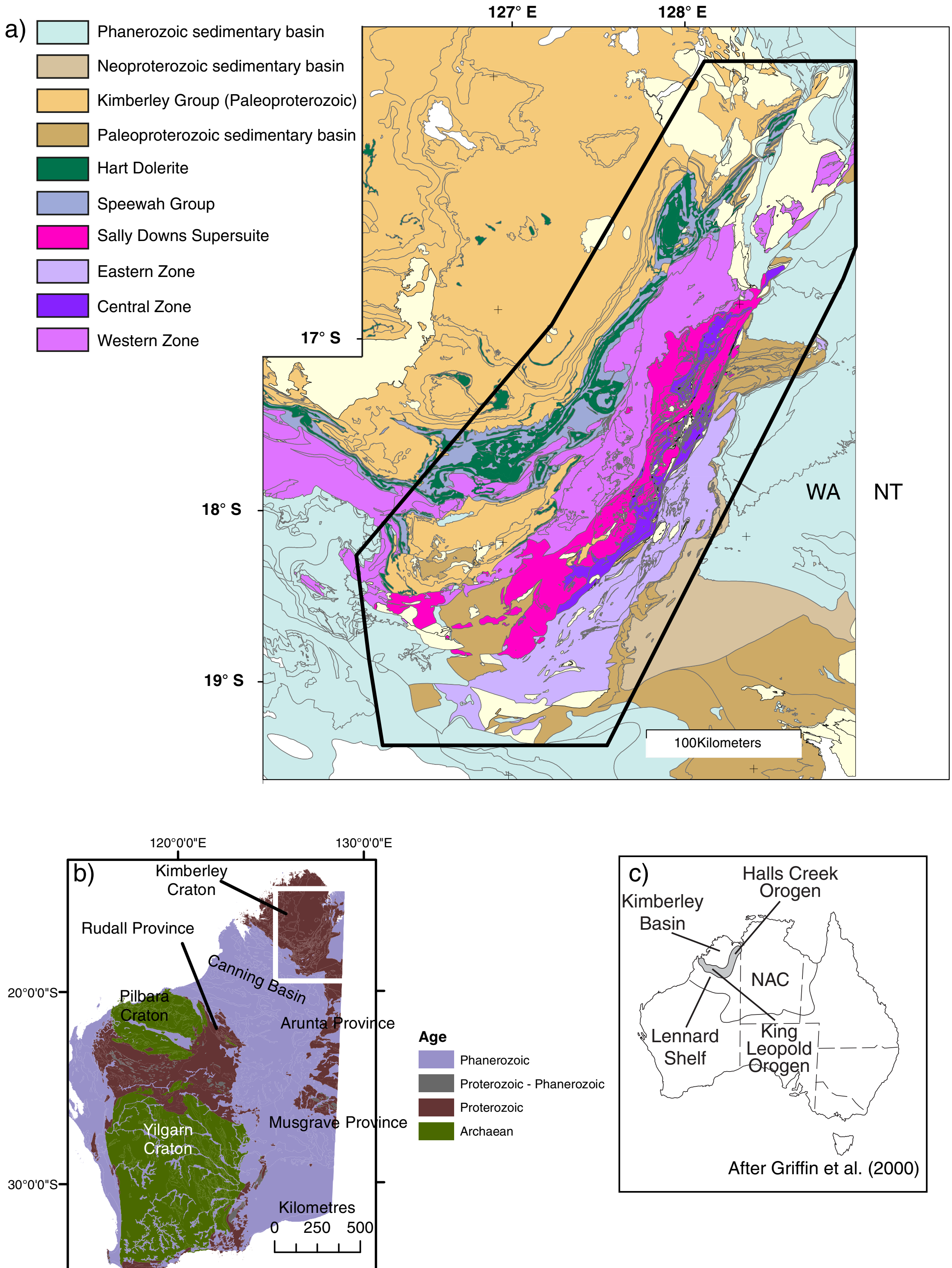

Fig. 1. a. Map of the Eastern Lamboo Complex illustrating the presence and extent of the western, central and eastern zones and stitching granites of the Sally Downs Supersuite across them; b. Location map of the Kimberley region with Australia; c. Illustration of the extent of the Lamboo Complex around the Kimberley Basin.

approach that is appropriate for a multi-commodity large-scale mineral systems analysis, using the features of deep crustal-scale architecture, fertility, geodynamic throttle and depositional site and, preservation. This approach recognises the complexity of ore deposit system models. However, it groups the most pertinent features of them and allows unusual or disparate mineralisation styles to be captured in a semi-automated prospectivity analysis, thus overlooking complex details within individual ore system models.

2. Mineral systems analysis

Mineral systems analysis involves understanding the geodynamic processes that are required to form and preserve ore deposits (Wyborn et al., 1994). By using a mineral systems approach, prospectivity for disparate commodites can be considered. These commodities may be present in deposits already known in the region; however, the analysis workflow can also target commodities unknown to the area.

Key controlling processes on the formation and preservation of mineral systems include large scale processes such as the secular evolution of the Earth, lithospheric controls on mineral enrichment, and geodynamic drivers (Cawood and Hawkesworth, 2013; Groves and Bierlein, 2007; McCuaig et al., 2010; McCuaig and Hronsky, 2014). Of these processes, lithospheric enrichment and geodynamic drivers are directly linked to plate tectonics and the kinematics of plate motion, that is related to formation and breakup of supercontinents (Cawood and Hawkesworth, 2013; Goldfarb et al., 2001). Mineralisation processes related to the secular evolution of the Earth require that some styles of ore deposits only formed during certain periods of the Earth's history (Cline et al., 2005; Leach et al., 2010). Lithospheric- or crustal-scale architecture can be mapped through analysis of gravity datasets as well as MT inversions (Lindsay et al., 2015a; Lindsay, 2006; Spratt et al., 2014, 2007). Other controlling processes, such as specific lithologies as mineralisation traps (e.g. carbonate-evaporate sequences) are also important (Cline et al., 2005; Leach et al., 2010). In addition the current-day level of crustal exposure (i.e. the upper, middle, or lower crust) as a proxy for factors that may influence the preservation of different styles of mineralisation must be considered (Fig. 2). These key drivers or critical factors are scale dependent. For regional to district scale mineral systems analysis and targeting, it can be difficult to determine depositional site information (Table 1) (McCuaig and Hronsky, 2014).

The Halls Creek Orogen hosts a variety of mineralisation styles, with few being mined, either currently or historically. The different styles of mineral deposits or occurrences documented in the Halls Creek Orogen include Au in the Paleoproterozoic rocks of eastern zone, Pb, Cu, Ag, Au, Sb (in the Paleoproterozoic central and western zones), diamonds in the central and eastern zones, and Pb–Zn in Devonian reef complexes overlying these zones (Sanders, 1999; Hassan, 2004).

2.1. Tectonic triggers, fertility and depositional site

The Halls Creek Orogen documents several periods of the diachronous assembly of the Paleoproterozoic supercontinent Nuna/Columbia through the Hooper and Halls Creek Orogenies and accretion of the central and eastern zones to the Kimberley Craton (Huston et al., 2012; Tyler et al., 2012) (Fig. 3). Effects of the assembly of the supercontinent Rodinia (1300–900 Ma; Li et al., 2008) may also be inferred from the intrusion of c. 1180 Ma alkaline rocks in the region that host the Argyle diamonds (Jaques and Milligan, 2004; Jaques et al., 1990). The Gondwana amalgamation contributed to the formation of the Devonian reefs and Phanerozoic basins in the region.

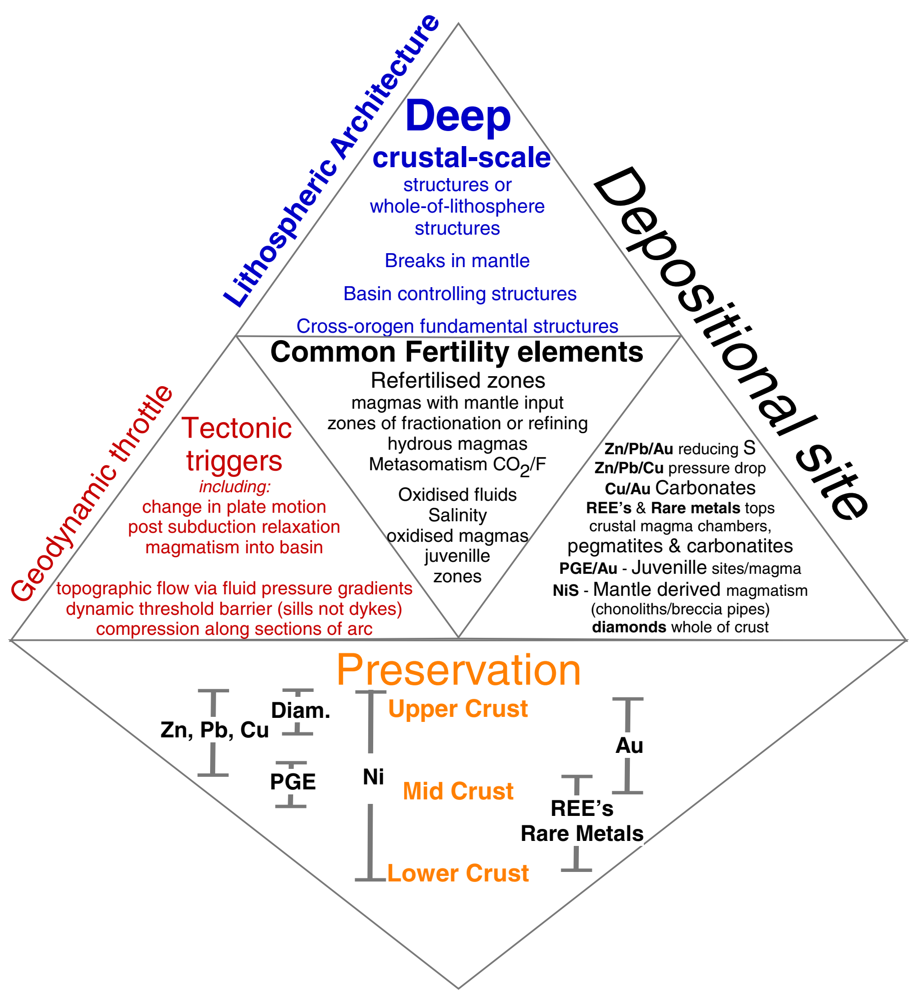

Fig. 2. Mineral Systems Diamond — a schematic diagram illustrating the main components required to form and preserve the listed mineral deposits, scale independent.

Table 1
Critical elements for the formation of gold deposits (modified from McCuaig and Hronsky, 2014).

	Critical elements for the formation of gold deposits			
	Fertility	Geodynamics	Architecture	Depositional zone
Deposit	*Not applicable*	*Not applicable*	Pipe-like rock volume most favorable for fracturing by fluid escape (either local structural complexity or pipe of more competent rock)	2nd order - region where there are pressure drops; 3rd order - favorable substrate (chemical scrubber)
Camp	*Not applicable*	Low active tectonic strain, ie. stress state causing fluid system to self-organise; areas of higher uplift favored, which provides stress switch and higher energy and mass transfer	Major heterogeneity perhaps manifested by intersecting structures, along trend of inverted rift-marginal faults that contain an appropriate physical seal (eg. antiform or unconformity)	1st order - upper 10 km of crust at the time of mineralisation where fluid pressure gradients are highest; preserved through any subsequent orogenic cycles
Province	Discrete Au-enriched upper lithospheric domain, particularly near province margin. Possible mantle-lithosphere enriched by small-volume partial melts prior to end of orogeny	Terminal phase of syn-orogenic event (eg. tectonic switch to incipient extension, post collision. If subduction - retreating oceanward)	Inverted retroarc rift, preferable formed at a continental margin, or over an old margin of deep mantle lithosphere 'vertically accretive' suture	*Not applicable*
Continental	Occurrence of the western United States Au superprovince suggests that controls at this scale exists	Major collisional orogenic event during an evolving accretionary orogen that terminates a long-lived (>200 Ma) accretionary orogen	Subcontinental scale lineament, representing long-lived zone of dislocation in an accretionary orogen. Could be an old 'vertically accretive' suture	*Not applicable*

Fertility, tectonic triggers (geodynamic throttle) and depositional regions of different mineral systems types are intrinsically linked to cycles of supercontinent assembly and breakup (Cawood and Hawkesworth, 2013; Groves and Bierlein, 2007). Specific triggers are required to form a mineral deposit (Fig. 2) (Wyborn et al., 1994), and could include subduction initiation, changes in plate motion, magmatism, compression along an arc section, topographic flow via fluid pressure gradients or a specific dynamic threshold barrier (e.g. sills as opposed to dykes (Garwin et al., 2005; Groves and Bierlein, 2007; Gurney et al., 2005; Leach et al., 2010, 2005; Loucks, 2014; McCuaig et al., 2010; McCuaig and Hronsky, 2014; Seat et al., 2007)). Fertility elements required for the development of valuable mineral or gem deposits could include magmas with mantle input, zones of repeated magmatic fractionation, hydrous magmas, CO_2 or F metasomatism possibly driven by magmatic

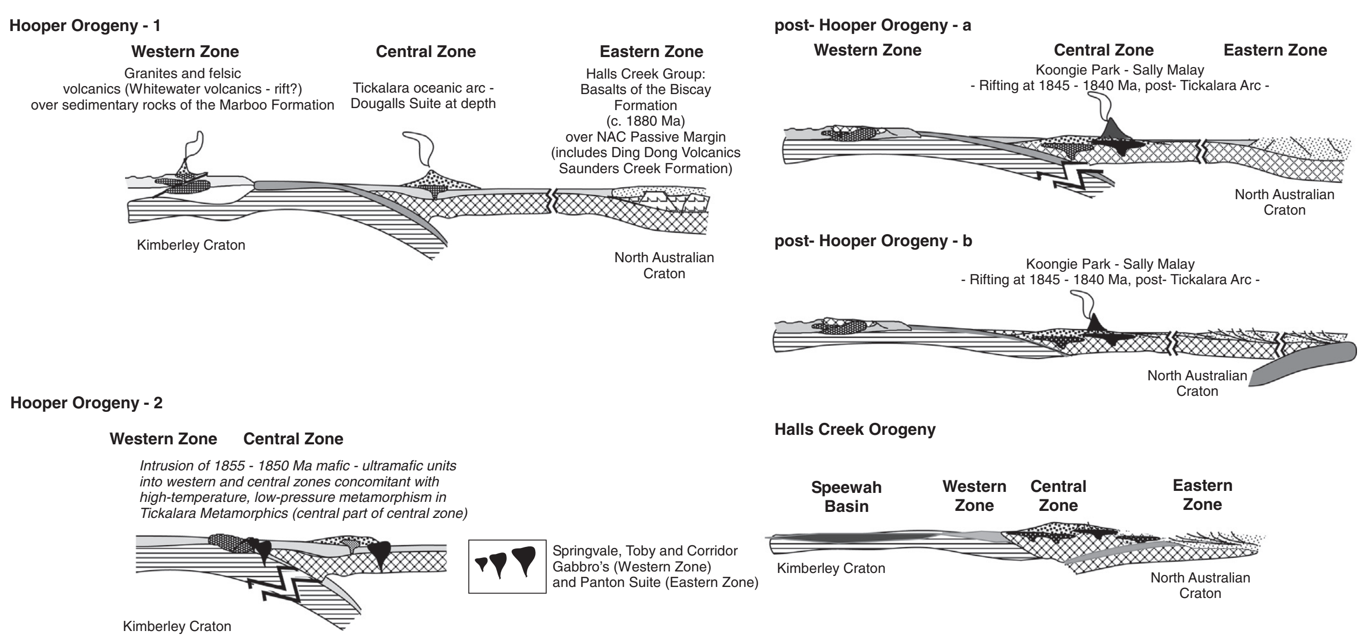

Fig. 3. Schematic diagrams illustrating the tectonic development of the Halls Creek Orogen from the Hooper Orogeny (1870–1850 Ma) to the end of the Halls Creek Orogeny (1835–1805 Ma). Hooper Orogeny — 1 and Hooper Orogeny — 2 depict start and end of the Hooper Orogeny; post-Hooper Orogeny — a and b depict different scenarios for the development of the Western, Central and Eastern Zones in the region at c. 1850 to 1840 Ma.

processes, salinity, oxidised fluids and oxidised or reduced magmas (Groves and Bierlein, 2007) (Fig. 2). Depositional sites are difficult to determine at a regional scale; however, they can include units such as mafic–ultramafic or alkaline magmas with juvenile input, or carbonate sedimentary rocks for base metal mineralisation.

Fertility and geodynamic throttle can be discussed in terms of three broad geological settings: Intraplate settings — e.g. basin formation (in extension and compression), extension and plate reorganisation during and after supercontinent assembly; interplate settings — e.g. convergence and transpressional setting — subduction and accretion of terranes, related to supercontinent assembly (e.g. Nuna/Columbia and Rodinia); and divergence and break up — e.g. rifting, formation of LIPs. In the Halls Creek Orogen, only two of these — intraplate and interplate settings have been noted (Tyler et al., 2012), within the context of more than two billion years (Tyler et al., 2012, Griffin et al., 2000; Sheppard et al., 1999; Hollis et al., 2014).

2.1.1. Geological evolution of the Halls Creek Orogen

The western, central and eastern zones of the Lamboo Province contain distinct geological units formed during the early Paleoproterozoic that originated in diverse tectonic settings, or at different times, suggesting that they were juxtaposed during regional-scale orogenesis (Figs. 1, 3 and 4; (Griffin et al., 2000; Page et al., 2001; Tyler and Griffin, 1990)). Turbidites of the Marboo Formation, exposed in the western zone, formed as a result of rifting of the Kimberly Craton after, c. 1870 Ma, based on the youngest detrital zircon populations within the sedimentary rocks, and the 1865–1850 Ma crystallisation age of intrusives and extrusives of the Paperbark Supersuite that

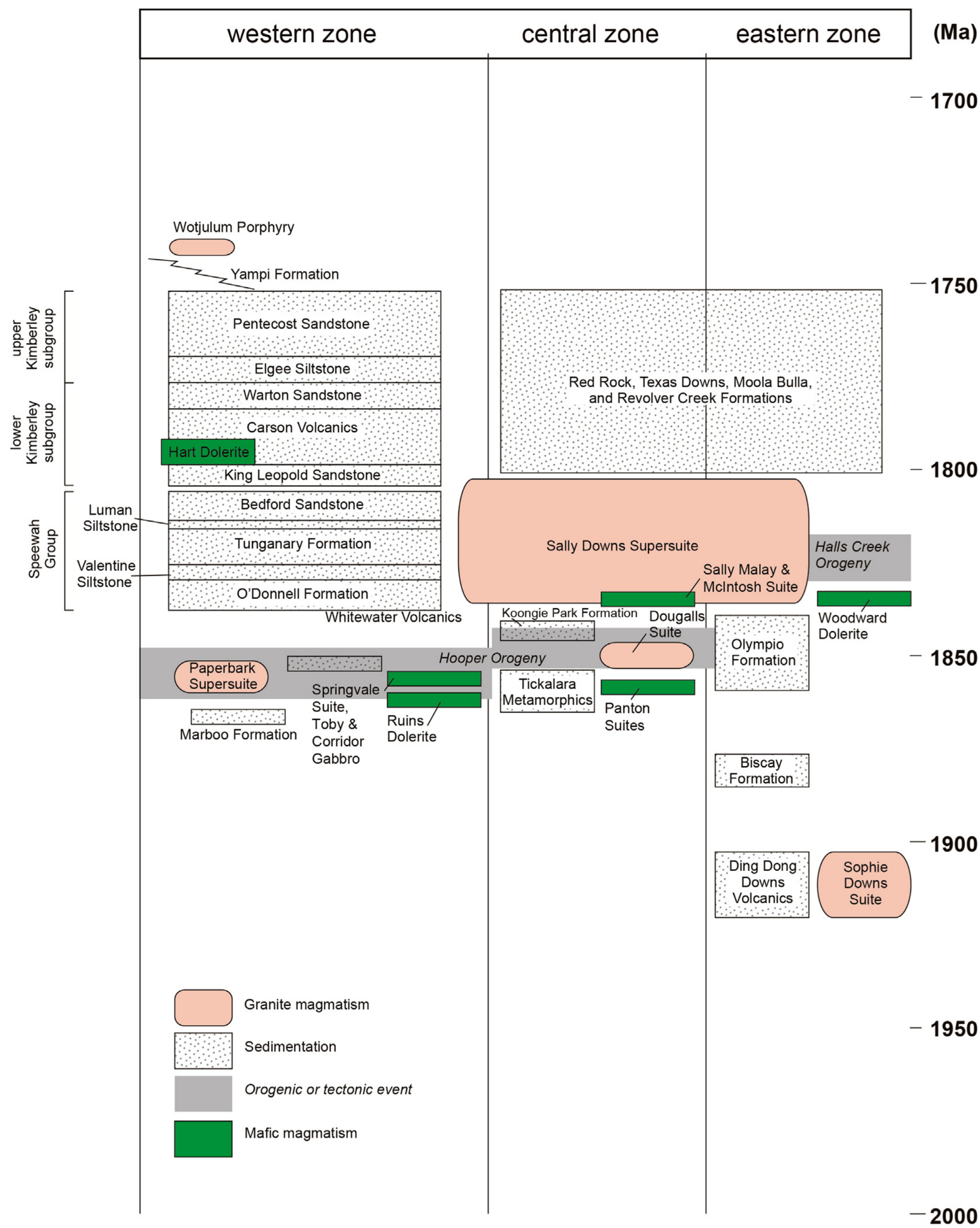

Fig. 4. Time-space plot illustrating the relative development of the Eastern, Central and Western zones of the Halls Creek Orogen — eastern Lamboo Province. Modified from Hollis et al. (2014).

intrudes them (Tyler et al., 1999; Griffin et al., 2000; Hollis et al., 2014; Sanders, 1999) (Fig. 4). The 1870–1850 Ma Hooper Orogeny only affected rocks in the western and central zones of the Lamboo Province, causing variable degrees of deformation and greenschist to granulite facies metamorphism (Sheppard et al., 1997; Tyler et al., 1999).

The central zone initially developed as an oceanic island arc — Tickalara Arc — at c. 1865 Ma (Figs. 3 and 4) over an easterly dipping subduction zone, outboard of the Kimberley Craton (Sheppard et al., 2001). Sedimentary rocks, mafic volcanic and volcaniclastic rocks of the Tickalara Arc were intruded by tonalite, trondhjemite, and diorite sheets of the juvenile Dougalls Suite (Sheppard et al., 2001). These rocks were deformed and metamorphosed at high temperature, low pressure amphibolite to granulite facies at 1865–1856 Ma, and 1850–1845 Ma, during and after the Hooper Orogeny (Blake et al., 2000; Bodorkos et al., 1999; Bodorkos and Reddy, 2004; Page et al., 2001).

Emplacement of the first layered mafic–ultramafic intrusive rocks into the western and central zones took place between 1859 and 1853 Ma (Fig. 4) (Hoatson and Blake, 2000). In the western zone intrusion of mafic–ultramafic rocks was partly contemporaneous with the emplacement of the Paperbark Supersuite as illustrated by the presence of net-vein, back-veining and pillow-style relationships (Blake et al., 2000). At the same time the layered mafic rocks of the c. 1857 Ma Springvale and c. 1855 Ma Toby intrusions (Hoatson, 2000) were emplaced into the Paperpark Supersuite and Marboo Formations. In the central zone, the contemporaneous c. 1856 Ma mafic–ultramafic Panton Suite intruded into the Tickalara Metamorphics (Fig. 4).

Cessation of the Hooper Orogeny resulted in rifting of the Tickalara Arc during a period of plate reorganisation between 1845 and 1840 Ma (Tyler et al., 2012) (Fig. 3), resulting in the emplacement of felsic and mafic volcanics and sedimentary rocks of the Koongie Park Formation, and layered mafic to ultramafic sills of the Sally Malay Suite (Figs. 3 and 4) (Sewell, 1999; Tyler et al., 2012). The supracrustal Koongie Park Formation is restricted to the central to southern part of the central zone whereas, the intrusive Sally Malay Suite is restricted to the northern part of the central zone — suggesting that later exhumation in the north was greater than in the south.

The eastern zone contains felsic and mafic volcanic rocks and sedimentary rocks that developed over a passive continental margin on the western margin of the North Australian Craton (Fig. 3) (Tyler et al., 2012). The oldest known rocks in the eastern zone are felsic and mafic volcanic rocks and associated granites of the c. 1910 Ma Ding Dong Downs Volcanics (Fig. 4). These were unconformably overlain by siliciclastic sedimentary and volcanic rocks of the Halls Creek Group between 1880 and 1847 Ma. The basal Halls Creek Group consists of Paleoproterozoic rocks of the largely siliciclastic Saunders Creek Formation that is overlain by c. 1880 Ma mafic volcanics of the Biscay Formation (Fig. 4). Transition from a passive to active margin setting within the eastern zone is recorded through the deposition of turbidites of the Olympio Formation over the Biscay Formation at c. 1850 Ma (Blake et al., 1999, 2000; Tyler et al., 2012). Intrusion of the Woodward Dolerite into the Halls Creek Group after c. 1850 Ma may indicate a period of relaxation and local extension (Fig. 4).

The 1835–1805 Ma Halls Creek Orogeny affected the eastern Lamboo Complex and reflects suturing of the Kimberley Craton and North Australian Craton (Tyler et al., 2012; Sheppard et al., 2001, 1999). At this time voluminous felsic to intermediate granites and mafic rocks of the Sally Downs Supersuite intruded into the region, and the mafic igneous c. 1830 Ma McIntosh Intrusion was emplaced in the central part of the central zone (Blake et al., 2000).

Granitic batholiths of the Sally Downs Supersuite (the Mabel Downs, Syenite Camp and Kevins Dams suites) have geochemical characteristics suggesting they formed in a subduction-zone setting, (Sheppard et al., 2001) (Fig. 3). The age of the supersuite is broadly concurrent with the early stages of the high-temperature, low-pressure Halls Creek Orogeny (Bodorkos and Reddy, 2004).

The Speewah Group siliciclastic sedimentary rocks and minor felsic volcanics were deposited over the Kimberley Craton towards the end of the Halls Creek Orogeny. Unconformably overlying the Speewah Group is the Kimberley Group, which was intruded by mafic rocks of the c. 1800 Hart Dolerite that is part of a large igneous province (LIP) (Sheppard et al., 2012). After the cessation of the Halls Creek Orogeny, sedimentary rocks were deposited across the region in a series of discrete depocentres (Hollis et al., 2014).

The Yampi Orogeny (<1000–800 Ma) in the Kimberley region took place during the late Mesoproterozoic and is related to the development of the supercontinent Rodinia. The occurrence of diamondiferous kimberlites and lamproites in the Halls Creek Orogen (Sanders, 1999), and particularly the Argyle lamproite dated at c. 1180 Ma, by K–Ar and Rb–Sr age dating (Jaques et al., 1986; Luguet et al., 2009), is coincident with event. Extensive basin formation during the development of Gondwana led to the deposition of carbonate and siliciclastic successions in a range of basins developed over the Kimberley Craton and Lamboo Complex.

2.2. Deep crustal-scale structures

Deep crustal-scale structures are understood to control lithospheric architecture and therefore influence the development and emplacement of a wide range of mineral deposits (Bierlein et al., 2006; Grauch et al., 2003; McCuaig et al., 2010; McCuaig and Hronsky, 2014; White et al., 2014; White and Muir, 1989). In some regions, disparate mineral deposits that formed in diverse tectonic settings and at vastly different times are present along, or adjacent to such fundamental structures (McCuaig and Hronsky, 2014; O'Driscoll, 1981). This suggests that these structures and their splays have an ongoing influence on fluid flux, and that understanding their evolution and kinematic history is essential (Lindsay et al., 2015a, 2015b, 2015c; Lindsay, 2006; McCuaig et al., 2010; McCuaig and Hronsky, 2014; O'Driscoll, 1981).

Crustal-scale structures are known to form in active continental and oceanic arc regions, subparallel and orthogonal to the advancing subduction zone (Garwin et al., 2005; Sillitoe, 2008; White et al., 2014), with the orthogonal structures interpreted to be transform faults. In these regions, porphyry and epithermal deposits appear to develop over deep-seated structures, particularly where they intersect each other as demonstrated in Southeast Asia and the West Pacific (Garwin et al., 2005; White et al., 2014). These types of structures are also present in intraplate regions as suture zones, which represent the old margins of continental lithospheric blocks formed during subduction (Gorczyk et al., 2013; O'Driscoll, 1981), where they are often located at former collision zones and occasionally adjacent to major strike-slip shear zones. For example, iron-oxide copper gold (IOCG) deposits in the Gawler Craton in South Australia formed where a west-dipping Paleoproterozoic subduction zone (Groves et al., 2010; Hayward and Skirrow, 2010) is intersected by orothogonal deep crustal-scale structures. Similarly, in the Musgrave Province Ni–Cu-PGE mineralisation occurs over a triple junction between the West Australian, North Australian, and South Australian Cratons (Fig. 1b and c) which corresponds to the intersection of the Musgrave thermal anomaly and the Mundrabilla Shear Zone (Gorczyk et al., 2013; Smithies et al., 2011; Smithies et al., 2015). In this case, the juxtaposition of different crustal blocks (with presumably contrasting lithospheric properties) by large strike-slip motions on the Mundrabilla Shear zone may be related to focusing mineralisation in the region (Smithies et al., 2015).

In the Halls Creek Orogen deep crustal-scale structures are recognised through analysis of gravity, magnetic, remote sensing and geological data (Lindsay et al., 2015b) (Fig. 5). Breaks in gravity data and changes in orientation of magnetic lineaments are taken as representing faults and shear zones (Lindsay et al., 2015b). In general terms, breaks in gravity data are taken as representing deeper structures than those observed in magnetic data, as magnetic data tend to only

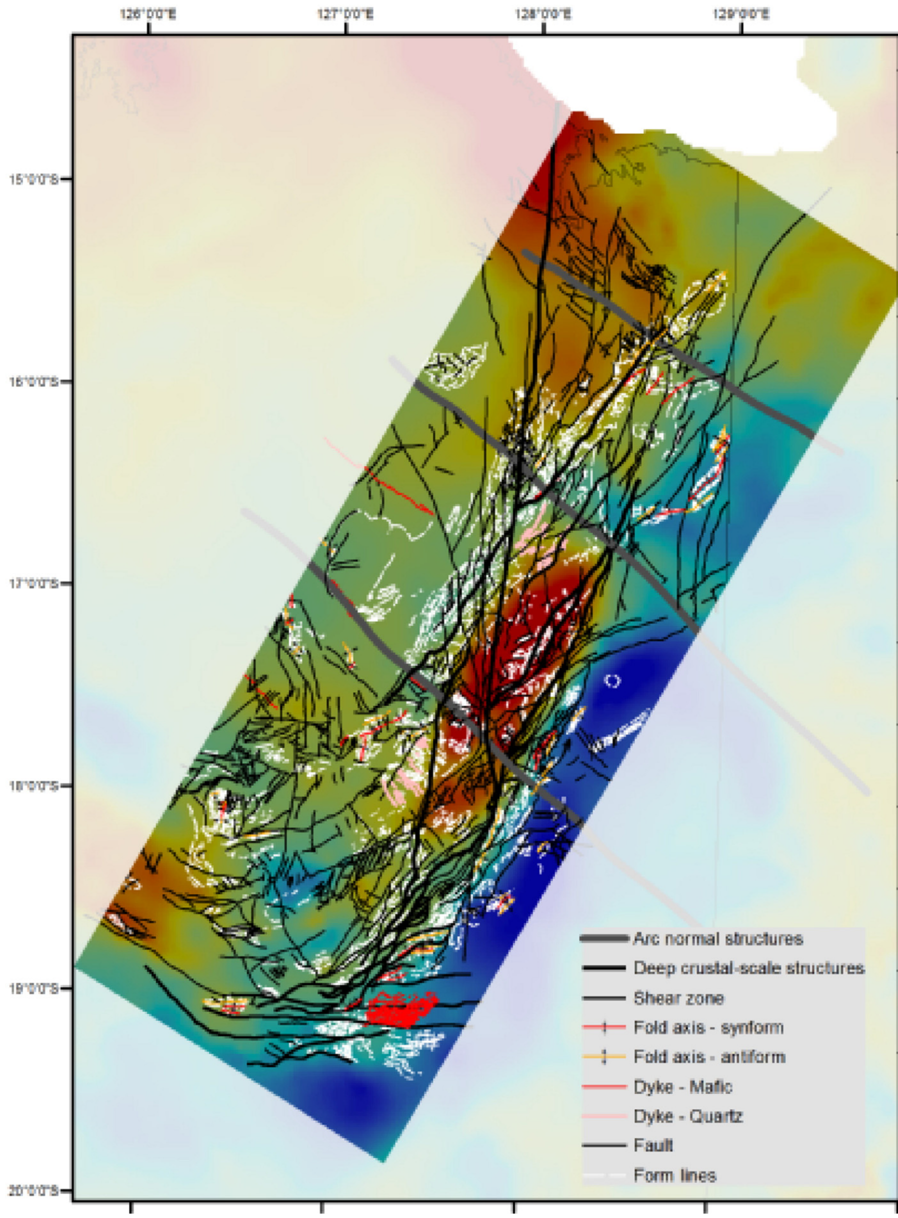

Fig. 5. Structural elements of the Halls Creek Orogen delineated from geophysical data and the geological and metamorphic maps overlain on a bouguer gravity image. From Lindsay et al. (2015b).

represent the upper to middle crust (down to c.10 km) (Lindsay et al., 2015b).

Three zones make up the Halls Creek Orogen — the western, central and eastern zones — and are separated by large-scale orogen-parallel faults or shear zones (Fig. 1). Although reactivated throughout the Paleoproterozoic, these boundaries formed through accretion and collisional processes (Sheppard et al., 2001, 1999,1999; Tyler et al., 2012, 2012; Blake et al., 2000; Lindsay et al., 2015b) (Fig. 3).

Orogen-normal, and some north-trending faults or shear zones cut through orogen-parallel faults and shears in the Halls Creek Orogen (Fig. 5). At the surface and subsurface orogen-normal structures are steep and locally form bounding structures to different lithological units within the western, central and eastern zones. Notably, these structures also separate units that have been metamorphosed at different temperatures and pressures, illustrating that they have facilitated vertical displacement (Lindsay et al., 2015b). This is especially obvious in the central part of the Halls Creek Orogen (Figs. 1 and 6) (Lindsay et al., 2015b). The age of orogen-normal faults and north-trending deep crustal-scale structures in the region is unknown. It is apparent that orogen-normal faults cut through the eastern zone, thus they were probably active during the Halls Creek Orogeny; however, analysis of Hooper Orogeny-aged metamorphism suggests that these structures may have been active during the Hooper Orogeny, as they are coincident with rock packages metamorphosed at different metamorphic grades and juxtaposed through faulting and shearing (Bodorkos and Reddy, 2004; Bodorkos et al., 2002; Lindsay et al., 2015b; Tyler et al., 1999, 2012).

Curiously, a c. 460 km long northerly trending, probably steep dipping deep crustal-scale sinistral shear zone with c. 10 km offset, cuts across the western, central and eastern terranes of the Halls Creek Orogen at about 128°E longitude (Fig. 6) (Lindsay et al., 2015b). The age of this structure is unknown; however, the strike-slip movement observed in the upper crust is probably post-Halls Creek Orogeny. Although the latest movement along the fault may be relatively young, within the region geological units proximal to the fault trend obliquely to the regional structural grain (usually NE — Halls Creek Orogen-parallel), and in some extreme cases their trend is subparallel to the shear zone (Lindsay et al., 2015a). This illustrates that this structure

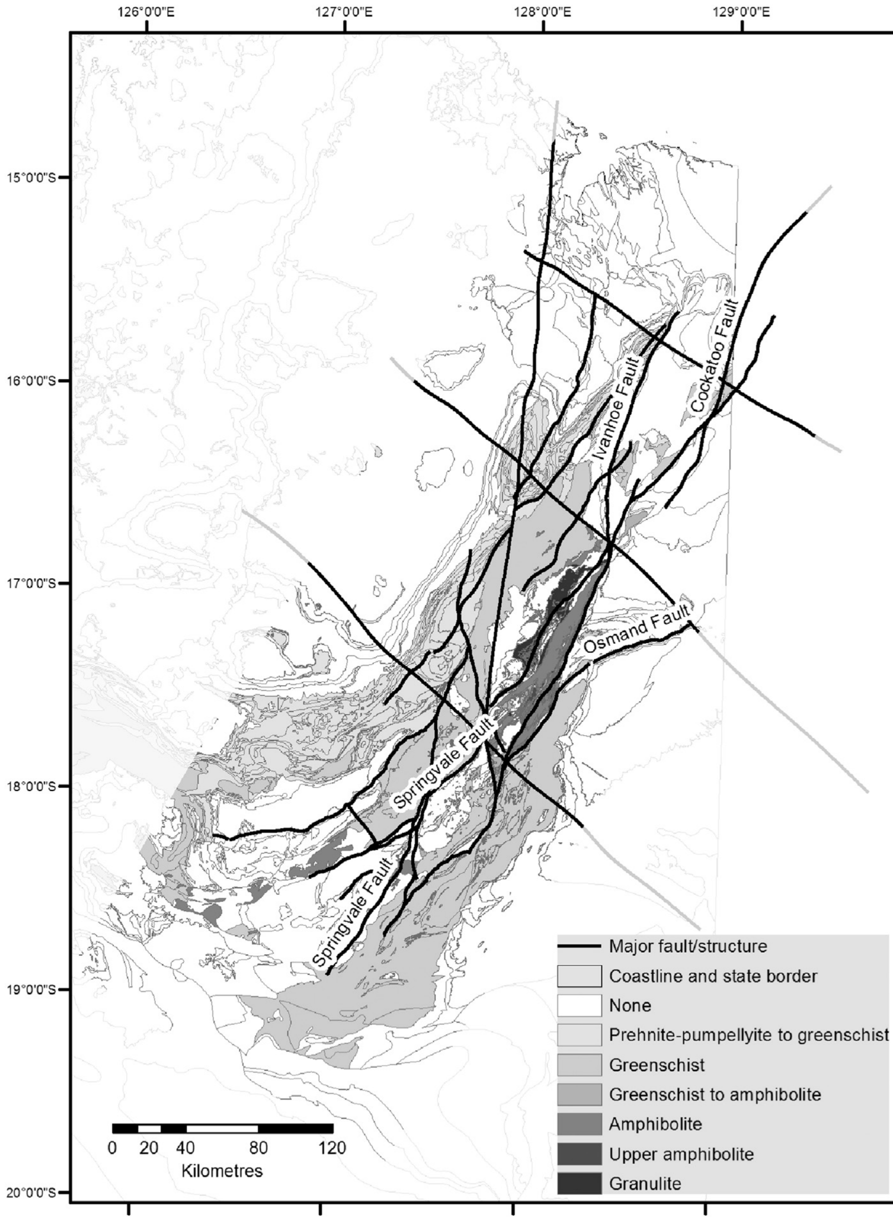

Fig. 6. Map of regional metamorphic grade of all units within the Halls Creek Orogen with structural-geophysical interpretation overlain. From Lindsay et al. (2015a, 2015b, 2015c).

has partly controlled the deposition and subsequent deformation of geological units forming within, or over it.

2.3. Mineral prospectivity associated with intraplate tectonics in the Halls Creek Orogen

The Marboo Formation, Amhurst Metamorphics, Paperbark Supersuite, Whitewater Volcanics, Halls Creek Group, Speewah Group, and Hart Dolerite all formed in intraplate settings or rift settings, and are prospective for a range of precious and base metal deposits as well as rare earths (Table 2).

2.3.1. Zn and Pb in sediment-hosted deposits

Zinc and Pb deposits are commonly found in sedimentary exhalative (SEDEX), clastic dominated (CD), evaporite replacement, and Mississippi-valley style deposits (Groves et al., 2010; Leach et al., 2010, 2005, 2013). Clastic dominated (CD) and SEDEX deposits form in a wide range of tectonic settings (Groves and Bierlein, 2007; Leach et al., 2010, 2005), and are preserved at a range of metamorphic grades (Huston et al., 2006; Leach et al., 2010). However, reactivation of deep-seated extensional faults, and close proximity to sutures between cratonic fragments may be necessary to form Pb–Zn deposits (Leach et al., 2005).

The Marboo Formation, of which the Amhurst Metamorphics are a high-metamorphic grade equivalent, was deposited between 1870 and 1865 Ma, in a rifted continental margin setting. The formation is prospective for Pb or Zn mineralisation of the CD — or SEDEX style of deposits as outlined by Leach et al. (2010). Within the eastern zone stratiform Cu–Pb–Zn (–Ag–Au) mineralisation occurs in the Biscay Formation (lower Halls Creek Group/Little Mount Isa prospect group including the Ilmars basemetal deposit) that formed in a passive continental margin over which sedimentary and mafic and felsic volcanics were deposited on the western margin of the North Australian Craton. Within the Biscay Formation, the most prospective intervals are felsic volcanic and volcaniclastic rocks interbedded with chemical sedimentary rocks (chert, BIF, carbonate, volcaniclastic rocks and siltstone) (Sewell, 1999).

The overlying Olympio Formation (upper part of the Halls Creek Group), which formed in a foreland basin setting to the Halls Creek

Table 2
Fuzzy inference network for Halls Creek Orogen prospectivity modelling. Note that the evidence weight, quoted in bold is the map weight * the confidence weight. For example, the map weight for the mantle tapping faults (0.9) * lithospheric architecture confidence (0.7) = 0.63; Num. classes — number of classes for a predictor map, Min. value — minimum class weight, Max. value — maximum class weight, Conf. fact. — confidence factor value for a predictor map, Fert. Weight — fertility map weight, Lith. Arch. Weight — lithospheric architecture map weight, Dep. site/geod. throt. weight — depositional site /geodynamic throttle map weight, Pres. weight — preservation weight.

		Buffer	Num. classes	Class. div.	Max. fav.	Min. fav.	Conf. fact.	Fert. weight	Lith. arch. weight	Dep. site /geod. throt. weight	Pres. weight	Fuzzy operator
Diamonds	Distance kimberlites lamproites (m)	15000	16	1000	1	0.001	0.9	0.81				**OR**
	Structural complexity crust (km^{-2})	NA	11	0.05	1	0.001	0.5	0.45				
	Distance major structures intersections (m)	10000	11	1000	1	0.001	0.9		0.63			**SUM**
	Distance major structures N (m)	10000	11	1000	1	0.001	0.9		0.63			**OR**
	Distance major structures NW (m)	10000	11	1000	1	0.001	0.8		0.56			
	Distance major structures NE (m)	10000	11	1000	1	0.001	0.7		0.49			
	Depth to moho (km)	NA	4	5	1	0.001	0.8			0.4		**OR**
	Central and Western Zone, Hart Dolerite, Speewah Group	10000	11	1	1	0.001	0.7			0.35		
Au	Woodward Dolerite (wd)	1000	3	1000	1	0.001	1.0	0.9				**OR**
	Dougalls Suite (DO)	1000	3	1000	1	0.001	1.0	0.9				
	Olympio Formation (HCo)	1000	3	1000	1	0.001	1.0	0.9				
	Biscay Formation (HCr-mkq, -xbb-cc)	1000	3	1000	1	0.001	1.0	0.9				
	Sally Downs Supersuite (SD-xgn-og, —md-mgt, —xgg-og)	1000	3	1000	1	0.001	1.0	0.9				
	Tickalara Metamorphics (Tl)	1000	3	1000	1	0.001	1.0	0.9				
	Koongie Park Formation (ke)	1000	3	1000	1	0.001	0.8	0.72				
	Biscay Formation (HCr-mf, -xmo-mg)	1000	3	1000	1	0.001	0.8	0.72				
	Sally Malay Suite (SM)	1000	3	1000	1	0.001	0.8	0.72				
	Hart Dolerite (ha)	1000	3	1000	1	0.001	0.6	0.54				
	Marboo Formation (mr)	1000	3	1000	1	0.001	0.6	0.54				
	Speewah Group (SP)	1000	3	1000	1	0.001	0.6	0.54				
	Sally Downs Supersuite (SD-xg-o)	1000	3	1000	1	0.001	0.6	0.54				
	Sophie downs Suite (SO)	1000	3	1000	1	0.001	0.6	0.54				
	Amhurst Metamorphics (am)	1000	3	1000	1	0.001	0.4	0.36				
Au	Distance major structures intersections (m)	10000	11	1000	1	0.001	0.9		0.63			**SUM**
	Distance major structures N (m)	10000	11	1000	1	0.001	0.9		0.63			**OR**
	Distance major structures NW (m)	10000	11	1000	1	0.001	0.8		0.56			
	Distance major structures NE (m)	10000	11	1000	1	0.001	0.7		0.49			
	Distance faults	5000	6	1000	1	0.001	0.6		0.42			
	Fault bends density (km^{-2})	NA	11	0.015	1	0.001	0.9			0.45		**OR**
	Fault intersection density (km^{-2})	NA	11	0.005	1	0.001	0.8			0.4		
	Structural complexity (km^{-2})	NA	11	0.2	1	0.001	0.8			0.4		
	Geochemical reactivity contrast	NA	11	0.2	1	0.001	0.8			0.4		
	Rhelological contrast	NA	11	0.2	1	0.001	0.8			0.4		
	Distance to fold axes (m)	5000	6	1000	1	0.001	0.7			0.35		
	Metamorphic zones	NA	4	NA	1	0.001	0.7				0.35	
Ni, Cu, Ti, V, PGE	Sally Malay Suite (SM-ap)	1000	3	1000	1	0.001	1.0	0.9				**OR**
	Panton Suite (PT)	1000	3	1000	1	0.001	1.0	0.9				
	Paperbark Supersuite (PB)	1000	3	1000	1	0.001	0.8	0.72				
	Sally Malay Suite (SM-ogn, -xo-a)	1000	3	1000	1	0.001	0.8	0.72				
	Lamboo Province ultramafic (ap-LM)	1000	3	1000	1	0.001	0.8	0.72				
	Hart Dolerite (ha)	1000	3	1000	1	0.001	0.6	0.54				
	Lamboo Province mafic–ultramafic (xo-a-LM)	1000	3	1000	1	0.001	0.6	0.54				
	Sally Downs Supersuite (SD)	1000	3	1000	1	0.001	0.2	0.18				
	Tickalara Metamorphics (Tl)	1000	3	1000	1	0.001	0.2	0.18				
	Distance major structures intersections (m)	10000	11	1000	1	0.001	0.9		0.63			**SUM**
	Distance major structures N (m)	10000	11	1000	1	0.001	0.9		0.63			**OR**
	Distance major structures NW (m)	10000	11	1000	1	0.001	0.8		0.56			
	Distance major structures NE (m)	10000	11	1000	1	0.001	0.7		0.49			
	Fault bends density (km^{-2})	NA	11	0.015	1	0.001	0.9			0.45		**OR**
	Fault intersection density (km^{-2})	NA	11	0.005	1	0.001	0.8			0.4		
	Structural complexity (km^{-2})	NA	11	0.2	1	0.001	0.8			0.4		
Cu, Au, Mo	Sally Downs Supersuite (SD)	1000	3	1000	1	0.001	0.4	0.36				**OR**
	Speewah Group (SP)	1000	3	1000	1	0.001	0.2	0.18				
	Hart Dolerite Granophyre (ha)	1000	3	1000	1	0.001	0.2	0.18				
	Angelo Microgranite (kn)	1000	3	1000	1	0.001	0.8	0.72				
	Syenite Camp Suite (SDS)	1000	3	1000	1	0.001	1.0	0.9				
	Whitewater Volcanics (PBww)	1000	3	1000	1	0.001	0.5	0.45				
	Distance major structures intersections (m)	10000	11	1000	1	0.001	0.9		0.63			**SUM**
	Distance major structures N (m)	10000	11	1000	1	0.001	0.9		0.63			**OR**
	Distance major structures NW (m)	10000	11	1000	1	0.001	0.8		0.56			
	Distance major structures NE (m)	10000	11	1000	1	0.001	0.7		0.49			
	Distance faults (m)	5000	6	1000	1	0.001	0.6		0.42			
	Fault intersection density (km^{-2})	NA	11	0.005	1	0.001	0.8			0.4		**OR**
	Structural complexity (km^{-2})	NA	11	0.2	1	0.001	0.8			0.4		
	Rheological contrast	NA	11	0.2	1	0.001	0.8			0.4		
	Metamorphic zones	NA	3	NA	1	0.001	0.7				0.35	
REE	Copperhead Igneous Complex (ch)	1000	3	1000	1	0.001	1.0	0.9				**OR**

Table 2 (*continued*)

		Buffer	Num. classes	Class. div.	Max. fav.	Min. fav.	Conf. fact.	Fert. weight	Lith. arch. weight	Dep. site /geod. throt. weight	Pres. weight	Fuzzy operator
	Olympio Formation (Hco-xmf-m)	1000	3	1000	1	0.001	1.0	0.9				
	Red Rock Formation (rk)	1000	3	1000	1	0.001	1.0	0.9				
	Olympio Formation (Hco-xsn-fn, -mft, -mf)	1000	3	1000	1	0.001	0.8	0.72				
	Granite in Eastern Zone (gnl-LM)	1000	3	1000	1	0.001	0.5	0.45				
	Eastman Granite (ea)	1000	3	1000	1	0.001	0.5	0.45				
	San Sou Monzogranite (ss)	1000	3	1000	1	0.001	0.5	0.45				
	Syenite Camp suite (SDS)	1000	3	1000	1	0.001	0.5	0.45				
	Sophie Downs Suite (SO)	1000	3	1000	1	0.001	0.3	0.27				
	Distance major structures intersections (m)	10000	11	1000	1	0.001	0.9		0.63			**SUM**
	Distance major structures N (m)	10000	11	1000	1	0.001	0.9		0.63			**OR**
	Distance major structures NW (m)	10000	11	1000	1	0.001	0.8		0.56			
	Distance major structures NE (m)	10000	11	1000	1	0.001	0.7		0.49			
REE	Fault bends density (km^{-2})	NA	11	0.015	1	0.001	0.9			0.45		**OR**
	Fault intersection density (km^{-2})	NA	11	0.005	1	0.001	0.8			0.4		
	Structural complexity (km^{-2})	NA	11	0.2	1	0.001	0.8			0.4		
	Metamorphic zones	NA	4	NA	1	0.001	0.7				0.35	
Sn, W, Mo	Paperbark Supersuite (PB)	1000	3	1000	1	0.001	1	0.9				**OR**
	Olympio Formation (HCo)	1000	3	1000	1	0.001	0.8	0.72				
	Granite in Eastern zone (gnl-LM)	1000	3	1000	1	0.001	0.5	0.45				
	Copperhead Igneous Complex (ch)	1000	3	1000	1	0.001	0.5	0.45				
	Sophie Downs Suite (SO)	1000	3	1000	1	0.001	0.3	0.27				
	Distance major structures intersections (m)	10000	11	1000	1	0.001	0.9		0.63			**SUM**
	Distance major structures N (m)	10000	11	1000	1	0.001	0.9		0.63			**OR**
	Distance major structures NW (m)	10000	11	1000	1	0.001	0.8		0.56			
	Distance major structures NE (m)	10000	11	1000	1	0.001	0.7		0.49			
	Distance faults	5000	6	1000	1	0.001	0.6		0.42			
	Fault bends density (km^{-2})	NA	11	0.015	1	0.001	0.9			0.45		**OR**
	Fault intersection density (km^{-2})	NA	11	0.005	1	0.001	0.8			0.4		
	Structural complexity (km^{-2})	NA	11	0.2	1	0.001	0.8			0.4		
	Geochemical reactivity contrast	NA	11	0.2	1	0.001	0.8			0.4		
	Distance to high K threshold boundary	5000	6	1000	1	0.001	0.8			0.4		
	Metamorphic zones	NA	4	NA	1	0.001	0.7				0.35	
Pb, Zn, Cu, Ag	Langfield Group (C-LA)	1000	3	1000	1	0.001	1	0.9				**OR**
	Ningbing Group (D-NI)	1000	3	1000	1	0.001	1	0.9				
	Koongie Park Formation (ke)	1000	3	1000	1	0.001	1	0.9				
	Biscay Formation (HCr)	1000	3	1000	1	0.001	0.7	0.63				
	Speewah Group (SP)	1000	3	1000	1	0.001	0.6	0.54				
	Amhurst Metamorphics (am)	1000	3	1000	1	0.001	0.5	0.45				
	Bungle Bungle Dolomite (uu)	1000	3	1000	1	0.001	0.5	0.45				
	Galloping Creek Formation (D-Co)	1000	3	1000	1	0.001	0.5	0.45				
	Marboo Formation (mr)	1000	3	1000	1	0.001	0.5	0.45				
	Winnama Formation (wi)	1000	3	1000	1	0.001	0.5	0.45				
	Hart Dolerite (ha)	1000	3	1000	1	0.001	0.4	0.36				
	Tickalara Metamorphics (Tl)	1000	3	1000	1	0.001	0.3	0.27				
	Carson Volcanics (KMc)	1000	3	1000	1	0.001	0.3	0.27				
	Olympio Formation (HCo)	1000	3	1000	1	0.001	0.1	0.09				
	Distance major structures intersections (m)	10000	11	1000	1	0.001	0.9		0.63			**SUM**
	Distance major structures N (m)	10000	11	1000	1	0.001	0.9		0.63			**OR**
	Distance major structures NW (m)	10000	11	1000	1	0.001	0.8		0.56			
	Distance major structures NE (m)	10000	11	1000	1	0.001	0.7		0.49			
	Distance faults	5000	6	1000	1	0.001	0.6		0.42			
	Fault bends density (km^{-2})	NA	11	0.015	1	0.001	0.9			0.45		**OR**
	Fault intersection density (km^{-2})	NA	11	0.005	1	0.001	0.8			0.4		
	Structural complexity (km^{-2})	NA	11	0.2	1	0.001	0.8			0.4		
	Geochemical reactivity contrast	NA	11	0.2	1	0.001	0.8			0.4		
	Rhelological contrast	NA	11	0.2	1	0.001	0.8			0.4		
	Metamorphic zones	NA	4	NA	1	0.001	0.7				0.35	

Orogeny may also be prospective for sediment-hosted Pb–Zn deposits (Tyler et al., 1990, 1999; Griffin et al., 2000; Hollis et al., 2014; Sanders, 1999), specifically over areas around deep crustal-scale structures that formed during, or prior to, the deposition of the Olympio Formation. Prospectivity within the Olympio Formation may be increased in rocks of a similar age to, or older than alkaline volcanic rocks within it (dated c. 1857 Ma, and c. 1848 Ma), which include the c. 1850 Ma trachyandesitic volcanic rocks of the Butchers Gully Member (Page and Sun, 1994).

Mississippi Valley-type (MVT) deposits are the dominant carbonate-hosted mineral systems in the both the west and east Kimberley, and in recent decades were mined on the Lennard Shelf (D'Ercole et al., 2000; Hassan, 2004). Most MVT deposits in the Lennard Shelf are proximal to fault-related dilation zones manifested through orthorhombic fault-fracture mesh (Dorling et al., 1996; Miller et al., 2007). In the northeast Kimberley the Sorby Hills deposits formed in lower Carboniferous carbonate reef complexes of the Burt Range Formation (Bonaparte Basin) on the eastern edge of a basement high — the Proterozoic Pincombe Inlier (Ferguson, 1999). Also in this region, the Devonian Ningbing reef complexes contain MVT style mineralisation that is preserved in a northwest trending horst block.

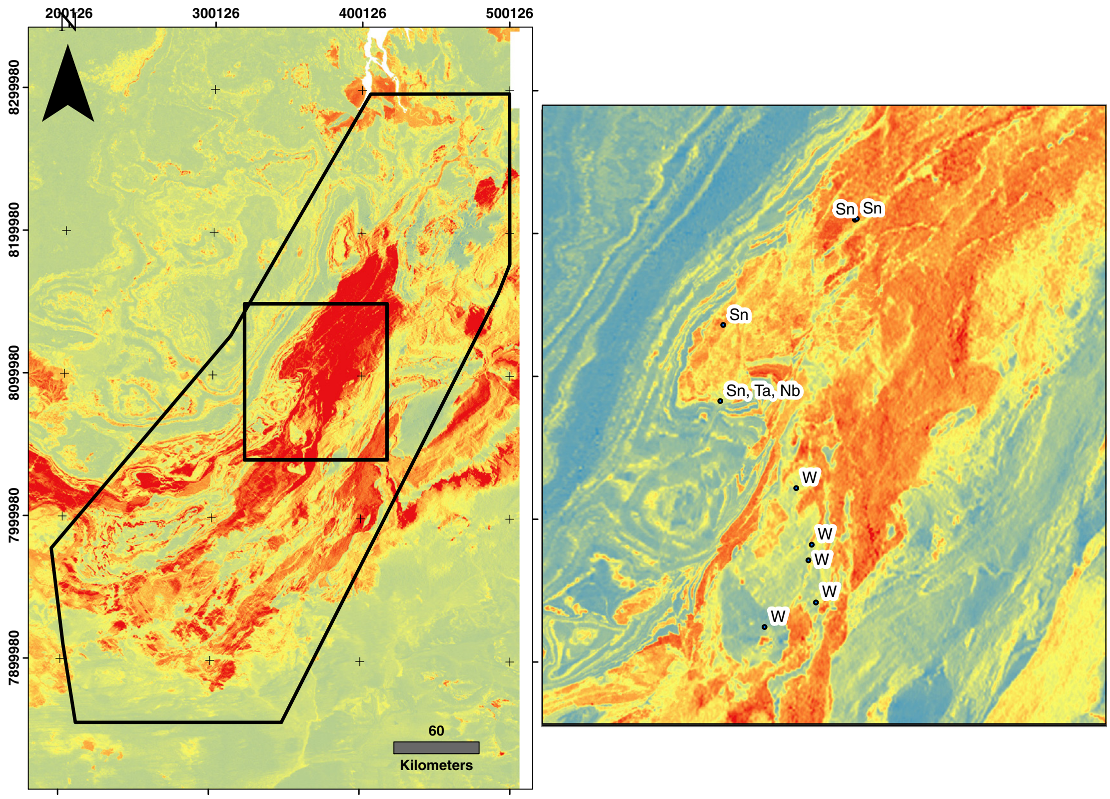

Fig. 7. Potassium radiometric image. Left — overlain by simplified deep crustal scale structures; right — Inset area overlain by W, Sn, Ta and Nb occurrences.

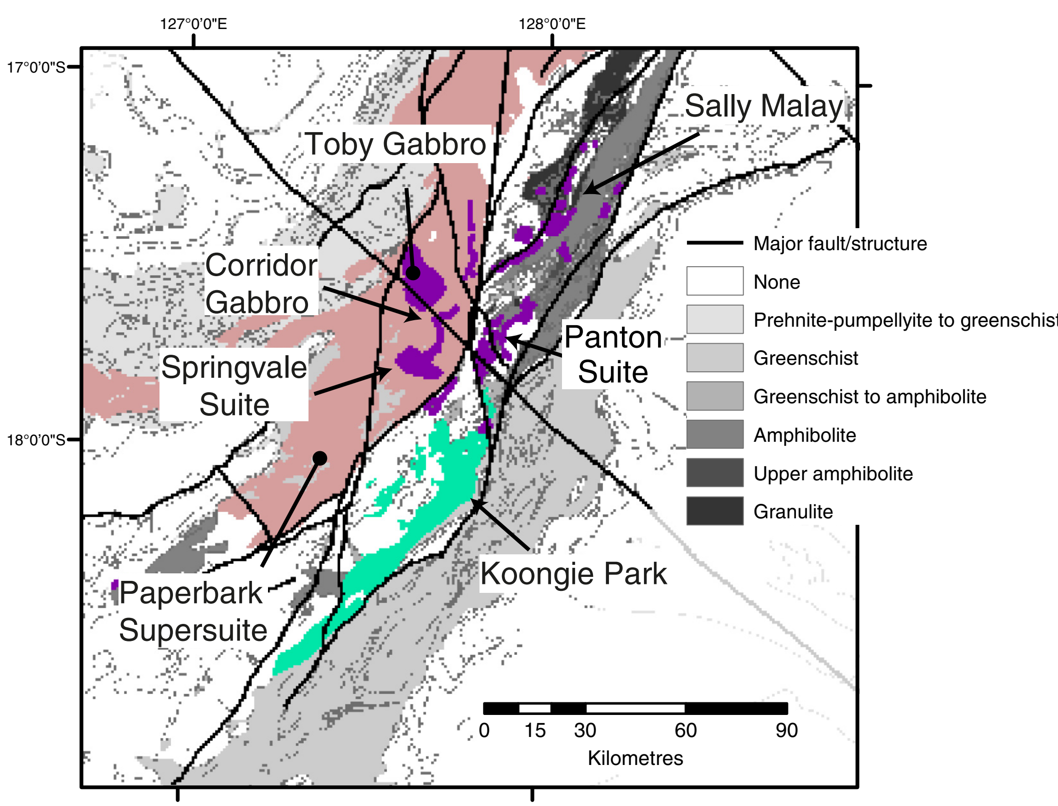

Fig. 8. Map illustrating the distribution of the Koongie Park Formation (light green), Sally Malay mafic-ultramafic intrusions (purple), Paperbark Supersuite (pink), and mafic to ultramafic rocks of the Corridor Gabbro, Sprinvale Suite, Panton Suite and Toby Gabbro (purple) in the eastern Lamboo Complex. (For interpretation of the references to colour in this figure legend, the reader is referred to the web version of this article.)

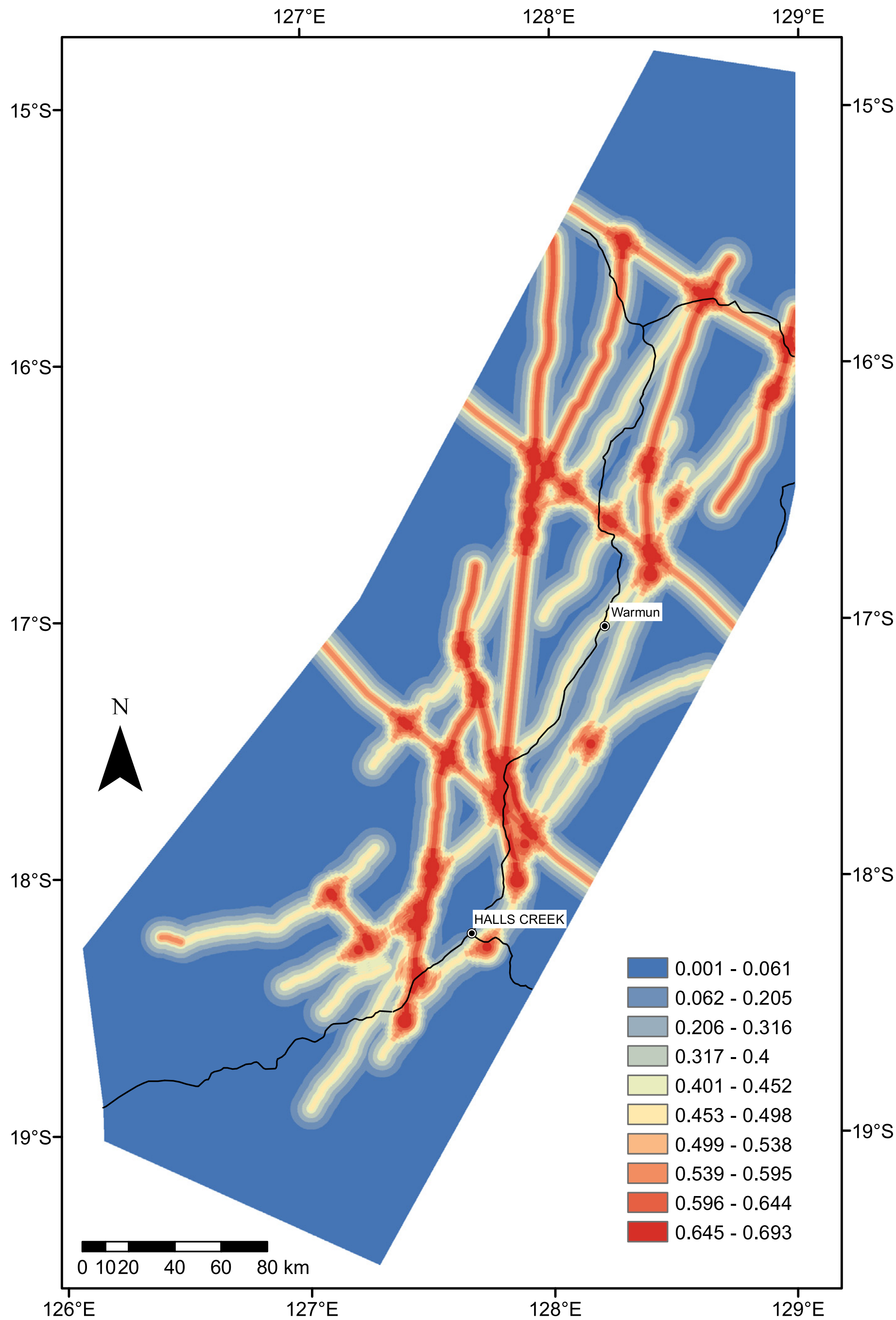

Fig. 9. Fuzzy crustal architecture intermediate map. A result of the fuzzy algebraic SUM of the distance to major faults and distance to their intersections.

2.3.2. Au, Ag, Cu, Zn, Sn, W in felsic to intermediate magmatic rocks and associated chemical sedimentary rocks

Granites and associated porphyries and volcanic rocks formed in the western and eastern zones of the Halls Creek Orogen during periods of rifting (Griffin et al., 2000; Sheppard et al., 2001). These include the Paperbark Supersuite, and possibly granites that form the basement to the Halls Creek Group in the eastern zone.

I-type granites, porphyries and volcanic rocks of the Paperbark Supersuite may be partly derived from melting of the sedimentary Marboo Formation (Griffin et al., 2000; Tyler et al., 2012) (Figs. 4 and 5). It is possible that the supersuite intruded into a zone of tensional stress into the Marboo Formation and therefore a region that had previously undergone rifting, thus the granites may be partly derived from melting of Marboo Formation rocks (Griffin et al., 2000). Additionally, based on whole-rock geochemical analysis Griffin et al. (2000) suggested that the granites formed by re-melting of older felsic rocks that formed over an early Proterozoic subduction zone, which Spratt et al. (2014) propose they detected in magnetotellurics data recently. Occurrences of Sn and W are known to occur in granite of the Paperbark Supersuite, whereas the volcanic component (Whitewater Volcanics) also reportedly contains occurrences of Nb, Pb, Cu, Mo, and Zn. The occurrences of Sn and W within Paperbark Supersuite granite are in a zone wedged between major north- and northwest-trending deep crustal scale structures. These appear to be alluvial occurrences. However, their distribution within and surrounded by rocks the K-rich granite of the Paperbark Supersuite suggests that they could be derived from it;

although this requires further investigation (Fig. 7). In the eastern zone, occurrences of Sn and W are associated with c. 1740 Ma pegmatite, veins of quartz, quartz-carbonate, quartz-tourmaline, and granite of the c. 1805–1790 Ma San-Sou Suite (Sanders, 1999). Many Sn–W occurrences in the eastern zone are associated with these occurrences of small late pegmatite dykes and granite stocks, that may have intruded late in, or after the Halls Creek Orogeny (Sanders, 1999).

The Nb, Pb, Cu, Mo, Zn metal association and tectonic setting of the Whitewater Volcanics suggests that mineralisation occurred in an epithermal rift-style setting west (inboard) of the Kimberley Craton margin (Sanders, 1999). Documented mineral occurrences are typically adjacent to faults that cut the Paperbark Supersuite, but may have been reactivated through time.

Metamorphosed sedimentary, and felsic and mafic volcanic rocks of the Koongie Park Formation are associated with massive sulphide mineralisation (Sewell, 1999) in the central zone (Fig. 8). Of particular interest are chemical sedimentary rocks of the Onedin Member of this formation. This formation was deposited between the Hooper and Halls Creek orogenies at 1845–1840 Ma, during a period of plate reorganisation, and possible local transtension. The development of the Koogie Park Formation over the Tickalara Arc, and in a region that has been mapped as containing significant deep crustal-scale structures suggests increased fertility in Cu, Pb, Zn, and Au (Tyler et al., 2012). Felsic porphyries in the region, such as the Angelo Microgranite, are subvolcanic equivalents to the Koongie Park Formation (Sanders, 1999) and are associated with Cu, Au mineralisation.

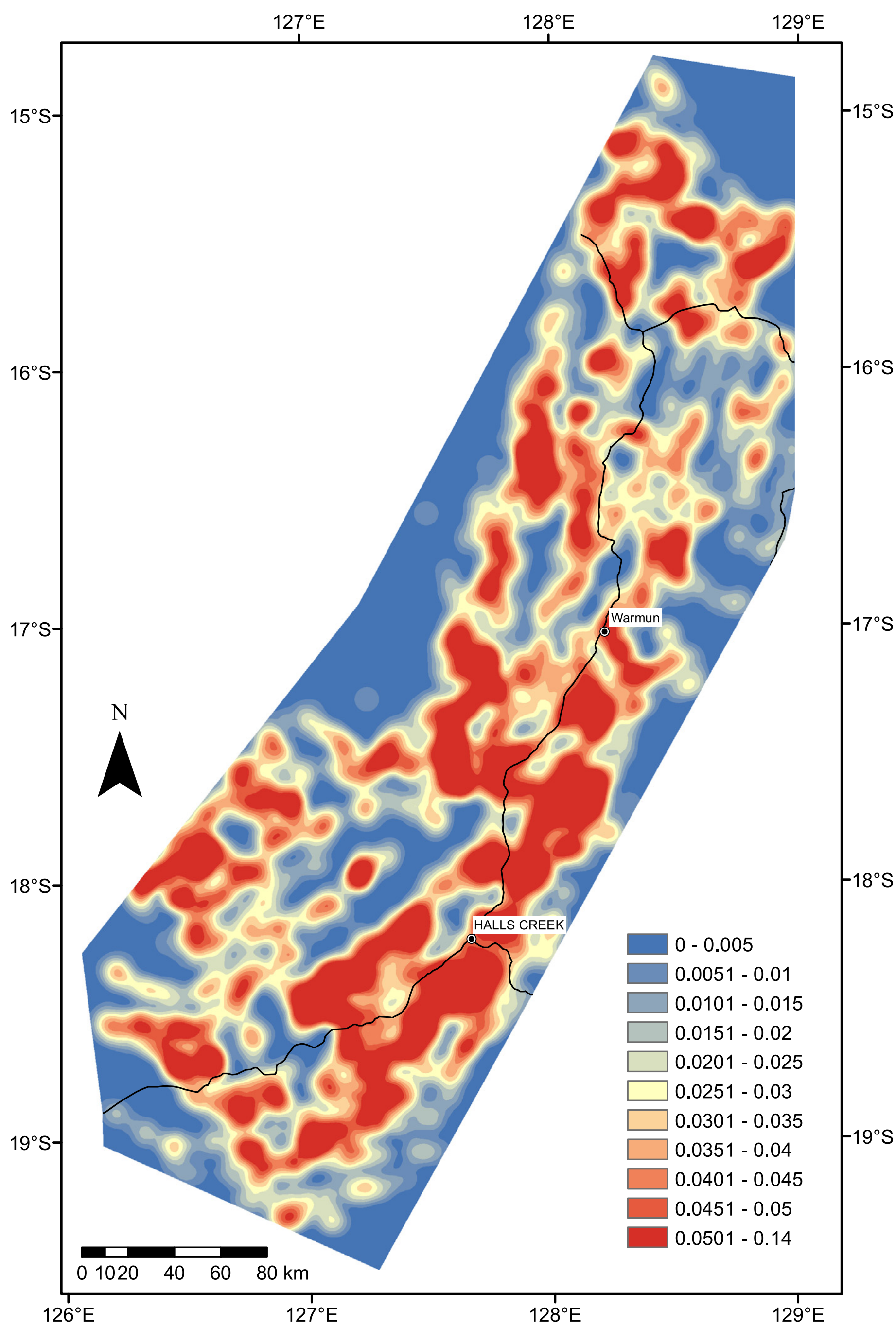

Fig. 10. Fault bends density calculated as kernel density.

2.3.3. Cu, Ni, PGE, V, Cr in mafic and ultramafic

Mafic and ultramafic rocks dated at c. 1850 Ma that both intruded and contain complex net-veining relationships with the Paperbark Supersuite formed in a transtensional setting (Figs. 5 and 8; Blake et al., 2000; Shaw et al., 2000; Hoatson and Lewis, 2014). These intrusive rocks include the Toby Gabbro, Corridor Gabbro and Springvale Suite that are spatially associated with northwesterly- and northerly-trending deep crustal scale structures (Lindsay et al., 2015b), suggesting these structures operated as a magma conduits. The Toby Gabbro and Springvale Suite are described as sub-horizontal sheet-like bodies (Shaw and Macias, 2000), or sills. No mineral deposits are known within these units; however, their mafic to ultramafic geochemistry, sill-like geometry, presence in a region around orogen-parallel and orogen-normal deep crustal-scale structures suggests that they may locally be associated with orthomagmatic Cu-PGE-V–Cr mineralisation (Fig. 8). Mafic–ultramafic layered intrusives of the c. 1856 Ma Panton Suite form a fault-bounded sequence in an area dominated by high metamorphic grade rocks (Tickalara Metamorphics). These are currently being mined at the Savannah NiS deposit.

The Sally Malay mafic–ultramafic intrusions are known to contain Ni, Cu and Co resources (Hoatson and Blake, 2000; Hoatson and Lewis, 2014). They are situated in a region around and within the Tickalara Metamorphics, which are proximal to large and deep crustal-scale structures (interpreted to be reverse faults). These faults are interpreted to have juxtaposed the granulite facies Tickalara Metamorphics rocks against lower metamorphic grade rocks (Fig. 8).

The c. 1790 Ma Hart Dolerite is a mafic intrusive sequence that forms a series of layered sills of dolerite and granophyre (Sheppard et al., 2012). The volume of the combined Hart Dolerite and Carson Volcanics is estimated to be c. 250,000 km^3 — which qualifies it as a large igneous province (Griffin et al., 1993; Sheppard et al., 2012). The Hart Dolerite is thought to have formed after the termination of the Halls Creek Orogen; perhaps, due to a period intraplate magmatism triggered by plate reorganisation (Tyler et al., 2012). Arndt et al. (2005) suggest that mafic magmas form in hot parts of the mantle, and although the processes that produce magmas endowed with ore elements are not clear-cut, their formation may be directly linked to contamination by sulphur-rich sedimentary country rocks, rather than interacting with sulphur sources at depth. The Hart Dolerite intrudes into sedimentary rocks of the Speewah Group and lower Kimberley Group and has significant outcrop at the southern and western margins of the Kimberley Basin. Indications that the Hart Dolerite has undergone some crustal contamination can be drawn from $^{143}Nd/^{144}Nd$ data taken from the granophyric portions (Sheppard et al., 2012) and the low Nb and Ta contents of the mafic units (Hollis et al., 2014).

The Hart Dolerite forms part of the north–northeast trending Speewah Dome, in the northern part of the western zone (Fig. 1). This area is host to Australia's largest magmatic V–Ti deposit (322mt @ 0.32%V_2O_5 and 2% Ti (King River Copper)). V–Ti in magnetite occur within differentiated gabbro within the upper parts of layered intrusive bodies. In lower parts of layered intrusives chromite and PGEs may accumulate (Groves and Bierlein, 2007). These rocks may also be host to Ni–Cu sulphides (Cawthorn, 1996). At Speewah Dome the V–Ti is hosted by titanomagnetite in a 100 m thick magnetite rich gabbro layer that is between a lower 300 m thick non-magnetic gabbro and overlying units of mafic to felsic granophyre. Within the magnetite gabbro, most mineralisation is in the lower 15–20 m with some accompanying increase in PGEs over 0.1 m (PGE + Au c. 700 ppb; Andrew et al., 2012; Hollis et al., 2014). South of Speewah Dome, low levels of PGEs in the Hart Dolerite sills, consistent with concentration of these elements in at least some late intrusive phases have been noted (Fiorentini, 2007).

2.3.4. Rare earth deposits associated with intrusive stocks

Rare earth element (REE) occurrences and deposits are mainly limited to the eastern zone and include the c. 1012–854 Ma Cummins range carbonatite complex (Downes et al., 2014), and small occurrences in the Olympio Formation (Halls Creek Group) associated with c. 1848 Ma alkaline volcanic rocks (Blake et al., 1999) at the Brockman prospect. One small occurrence in the central zone has been noted, Copperhead (Z52 377571E, 8041059N; Rugless and Pirajno, 1996). REE occurrences are known to be associated with deep crustal-scale structures and often magnetic anomalism, as is the case for the Cummins Range carbonatite complex (Downes et al., 2014); however, they are often associated with small stocks of alkaline intrusive rocks, and most commonly small carbonatites (London, 2011) that may not be represented on regional-scale maps.

2.3.5. Diamonds

The Kimberley region contains the highest known concentration of diamondiferous magmatic intrusions in Australia. These intrusions include kimberlites, lamproites, lamprophyres and carbonatites on, which range in age from 2020 to 20 Ma (Jaques and Milligan, 2004). Commercial diamonds in the Halls Creek Orogen are mined from a lamproite intrusion at Argyle (AK1 olivine-lamproite pipe, eastern margin of the central zone, Halls Creek Orogen) that has been reported as the only major diamond pipe known in an early Proterozoic orogenic belt (Luguet et al., 2009).

The c. 1180 Ma Argyle lamproite age (Jaques et al., 1986) (Luguet et al., 2009) overlaps with the formation of the supercontinent Rodinia, and the loosely constrained Yampi Orogeny (<1000–800 Ma) (Bodorkos and Reddy, 2004; Tyler and Griffin, 1990). Rhenium–Osmium (Re–Os) model ages for Argyle peridotite xenoliths contain a wide age range, from c. 1100 Ma to 3200 Ma, with the largest population being between 2900 Ma and 2200 Ma (Luguet et al., 2009), suggesting that the Argyle lamproite has intruded through Archean lithosphere, which is not exposed in the Halls Creek Orogen, but consistent with fast S-wave velocities down to c. 200 km reported for the region (Fishwick et al., 2005). These conditions are also consistent with the diamond stability field (5–5.9 GPa, 1140–1290 °C) (Jaques et al., 1990; Fishwick et al., 2005).

The location of Argyle is close to the intersection of a major northesast trending, and northwest trending, deep-crustal structures — which may have formed as early as the Paleoproterozoic during convergence and subduction at the Kimberley margin during the Halls Creek Orogeny (Gurney et al., 2010; Sanders, 1999).

2.4. Mineral prospectivity associated with interplate convergence tectonics in the Halls Creek Orogen

The upper plate of subduction zones are fertile for metals such as Cu, Au and Mo (Groves and Bierlein, 2007; Sillitoe, 2008). Rock units that

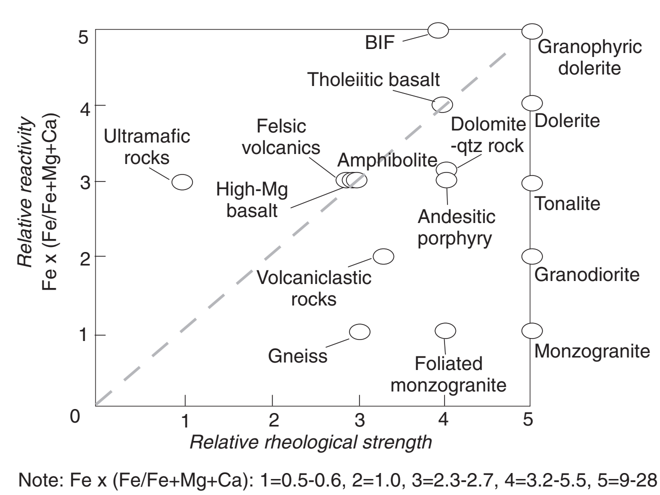

Fig. 11. Relative chemical reactivity and rheological strengths for selected rocks. Modified after Brown (2002).

developed during convergence and collisional processes in the Halls Creek Orogen include the following.

1. Protoliths to the Tickalara Metamorphics — mafic, sedimentary and granitic rocks that developed in the Tickalara Arc over an east dipping subduction zone during the Hooper Orogeny (Figs. 4 and 5).
2. Granitic and mafic rocks of the Sally Downs Supersuite that formed in an arc-type setting over a west dipping subduction zone during the Halls Creek Orogeny (Figs. 4 and 5).

Rocks that were deformed and metamorphosed during the Hooper or Halls Creek orogenies may be also be prospective for Au mineralisation (Groves and Bierlein, 2007) (Table 2). However, the formation and preservation of Au ore zones is most likely to be limited to low metamorphic grade domains (greenschist facies or lower).

2.4.1. Cu–Au–Mo in igneous rocks

Rocks formed in both the Tickalara and Sally Downs Arc during subduction may have generated porphyry and epithermal deposits prospective for Au, Cu and Mo (Sillitoe, 2008). The presence of major lithospheric-scale structures in these regions may both influence the fertility of the metal-bearing magmas (Loucks, 2014), and are required to focus the injection of Cu–(Au, Mo) fertile magmas into certain regions of the over-riding slab (Garwin et al., 2005; White et al., 2014).

Isotope values from some intermediate intrusives formed in the Tickalara Arc (Dougalls Suite) and the Sally Downs Arc (Mabel Downs and Sally Downs suites; Sally Downs Supersuite) contain high Sr/Y ratios above c. 40, and V/Sc values greater than c. 10 (see data in (Sheppard et al., 1997; Sheppard et al., 2001)). High Al_2O_3/TiO_2 (above c. 25) in the Mabel Downs and Syenite Camp suites suggest

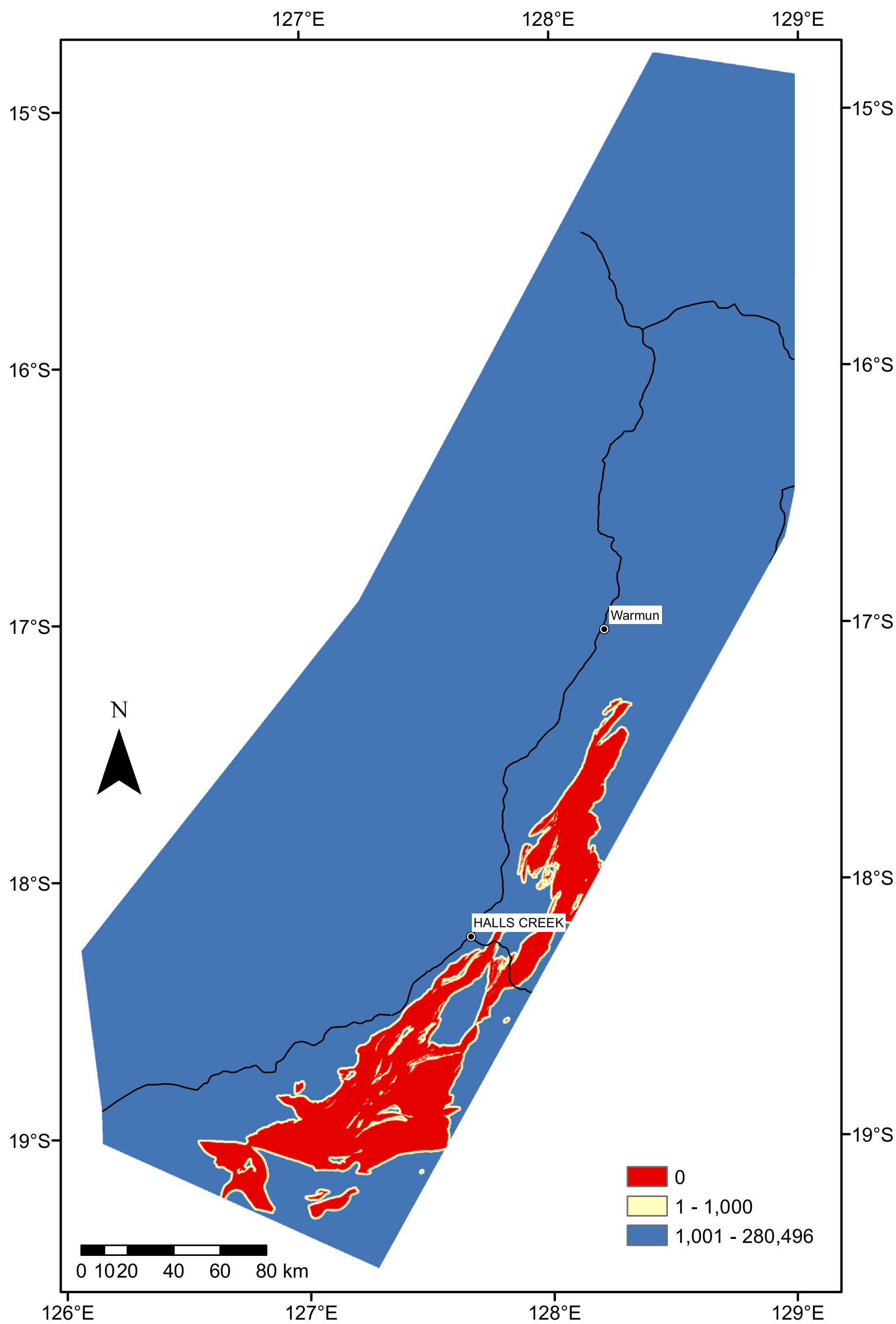

Fig. 12. Presence of the Olympio formation with a 1 km buffer used as fertility proxy to several mineral systems.

Table 3
Class values assigned to the metamorphic zones. Higher values correspond to higher prospectivity.

	Au	Cu, Au, Mo	Sn, W, Mo	REE	Zn, Pb, Cu
Granulite	0	0	0	0	0
Upper amphibolite	0	0	0	0	1
Amphibolite	0	0	0	0	1
Greenschist to amphibolite	1	0	1	1	1
Greenschist	3	1	3	3	2
Prehnite–pumpellyite to greenschist	2	2	2	2	2
None	1	2	1	1	3

the melts contain relatively high dissolved water, which is required for the formation of copper-ore-deposits (Loucks, 2014; Sheppard et al., 2001).

The Mabel Downs (Sally Downs Supersuite) and Dougalls Suites (Tickalara Metamorphics), have been metamorphosed to amphibolite facies (Bodorkos et al., 1999, 2002), or transitional greenschist-amphibolite facies (Sheppard et al., 2001). This suggests that if porphyry and epithermal deposits had formed in these rocks, they have either been exhumed and eroded or metamorphosed to higher grades. Were these upper crustal components preserved, they would be prospective for Cu, or Cu and Au porphyry related ores. Although the Syenite Camp Suite has not been metamorphosed throughout the region, upper crustal 'porphyry' parts to these intrusions have not been reported, suggesting that the rocks preserved may have formed at crustal

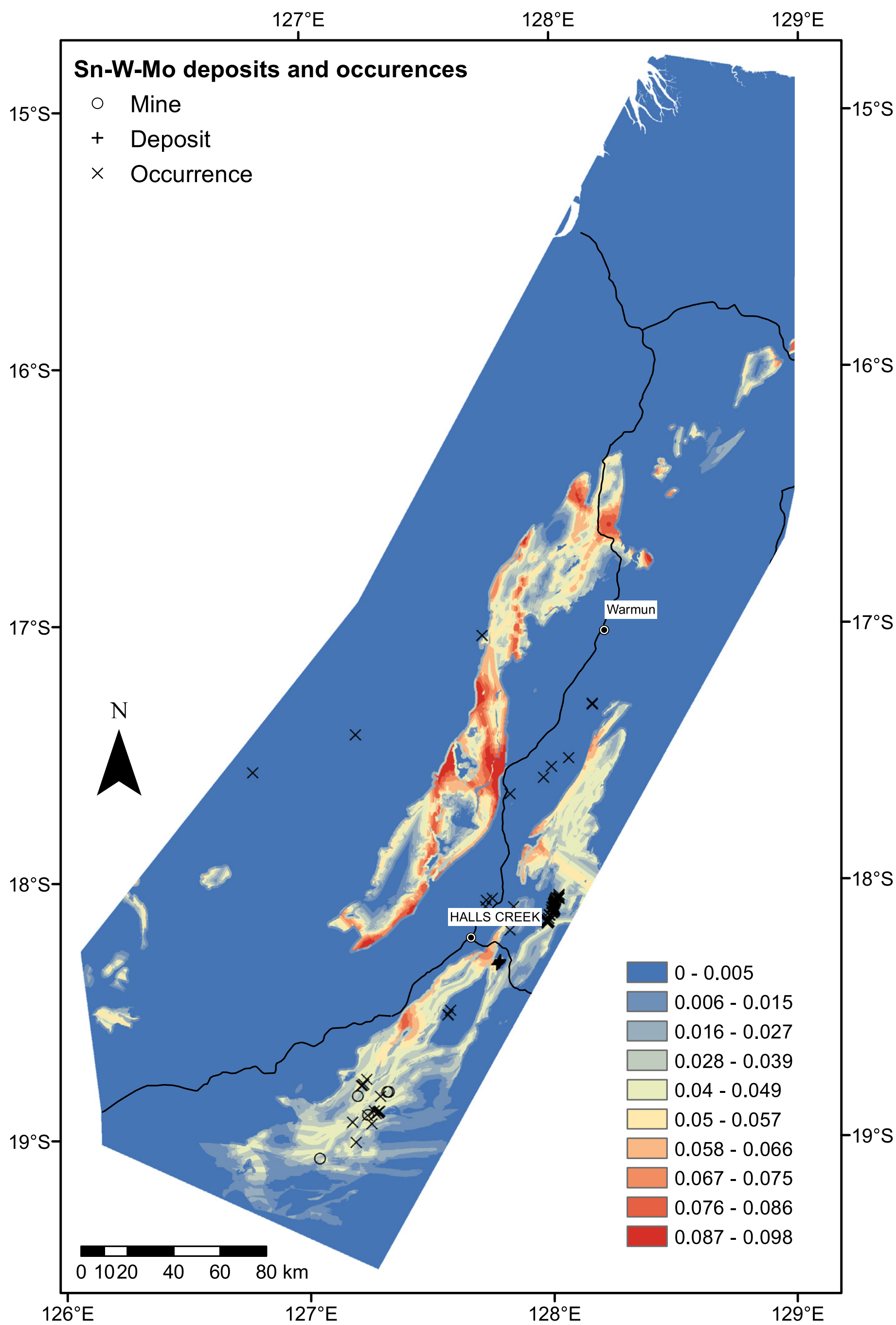

Fig. 13. Prospectivity map derived for Sn–W–Mo.

levels too deep for the formation and preservation of Cu-bearing porphyry style deposits, even if geochemical fertility indicators suggest that the magmas were Cu (–Au) fertile.

2.4.2. Au formed during orogenesis

In the eastern zone metamorphosed felsic volcanics, and sedimentary rocks in the Halls Creek Group are known to contain Au that probably formed sometime between 1810 Ma and 1780 Ma (Sanders, 1999), in the late stages of Halls Creek orogenesis, during, and subsequent to the accretion and collision of the eastern zone onto the central zone of the Halls Creek Orogen. Locally, in the southern parts of the central and western zones Au occurrences have been reported (Sanders, 1999). The accumulation of Au ore in the eastern zone is structurally controlled and often appears to be associated with fold hinge zones and kinks in the regional tectonic fabrics in the region, in a similar way to the occurrence of gold mineralisation in the Bendigo Goldfield in Victoria (Leader et al., 2013).

Location of mineralisation associated with orogenesis is commonly related to the presence of major long-lived crustal-scale structures, and particularly around areas where orogen-parallel and orogen-normal faults intersect (McCuaig and Hronsky, 2014). Above or around these major structures, deflection of the dominant regional structural grain may occur, leading to a marked difference in orientation of regional fold axial surfaces and foliations. Locations where features are oriented differently to the regional trends can reveal the location of dilational zones (fault jogs and/or pull apart structures) which can facilitate and focus ore-forming fluids (McCuaig and Hronsky, 2014), and providing a structural trap for the accumulation of ore. Structurally controlled Au

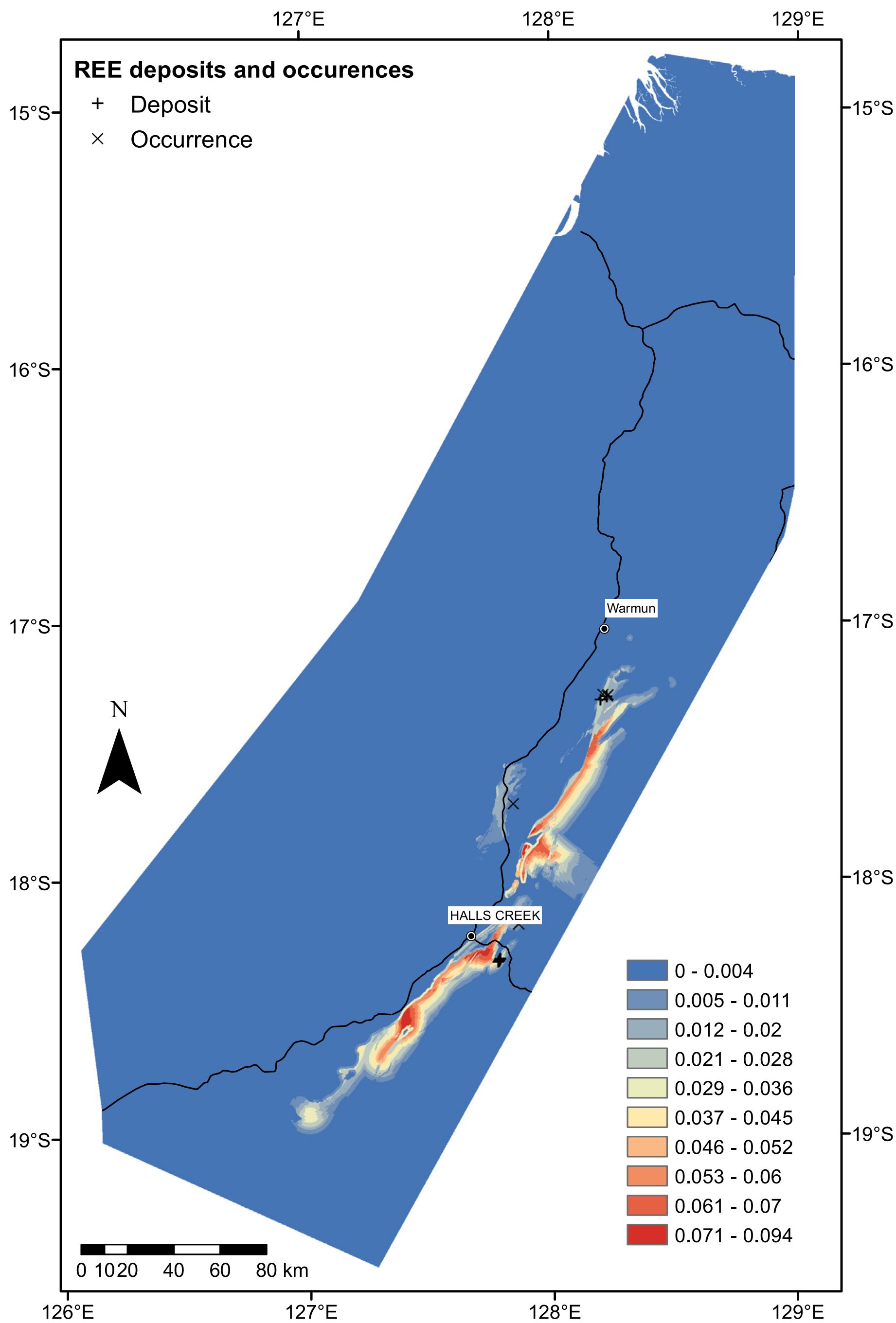

Fig. 14. Prospectivity map derived for REE.

mineralisation although mainly known in the Halls Creek Group, may is occur in any of the geological units formed prior to the Hooper or Halls Creek orogenies. However, this is most likely in regions that were metamorphosed in the greenschist facies, or lower and that are spatially adjacent to major lithospheric scale faults; even though preservation of Au deposits metamorphosed and deformed at high grade has been reported elsewhere (Tomkins and Grundy, 2009; Tomkins et al., 2009).

For example greenschist facies rocks of the Koongie Park Formation may be prospective for Au, especially in that the formation lies adjacent to major crustal scale faults that developed during the Halls Creek Orogeny (Lindsay et al., 2015b). This reasoning also holds for the Tickalara Metamorphics, Marboo Formation or other elements affected by orogenesis in the region.

2.5. Preservation

In the context of this work we mapped possible regions of preservation by using regional-scale metamorphic grade maps to represent proxies of crustal zones (lower, middle and upper; Fig. 6), and noted the presence of supracrustal versus intrusive rocks that formed at the same time in the region, but outcrop in different areas separated by faults (Fig. 8). Metamorphic maps illustrate that rocks metamorphosed under high temperature and relatively low pressure conditions outcrop in a northeasterly trending belt of the Tickalara Metamorphics in the central part of the central zone (Bodorkos et al., 1999, 2002; Lindsay et al., 2015b). These granulite facies rocks and migmatites were deformed and metamorphosed at temperatures of up to c. 800 °C and

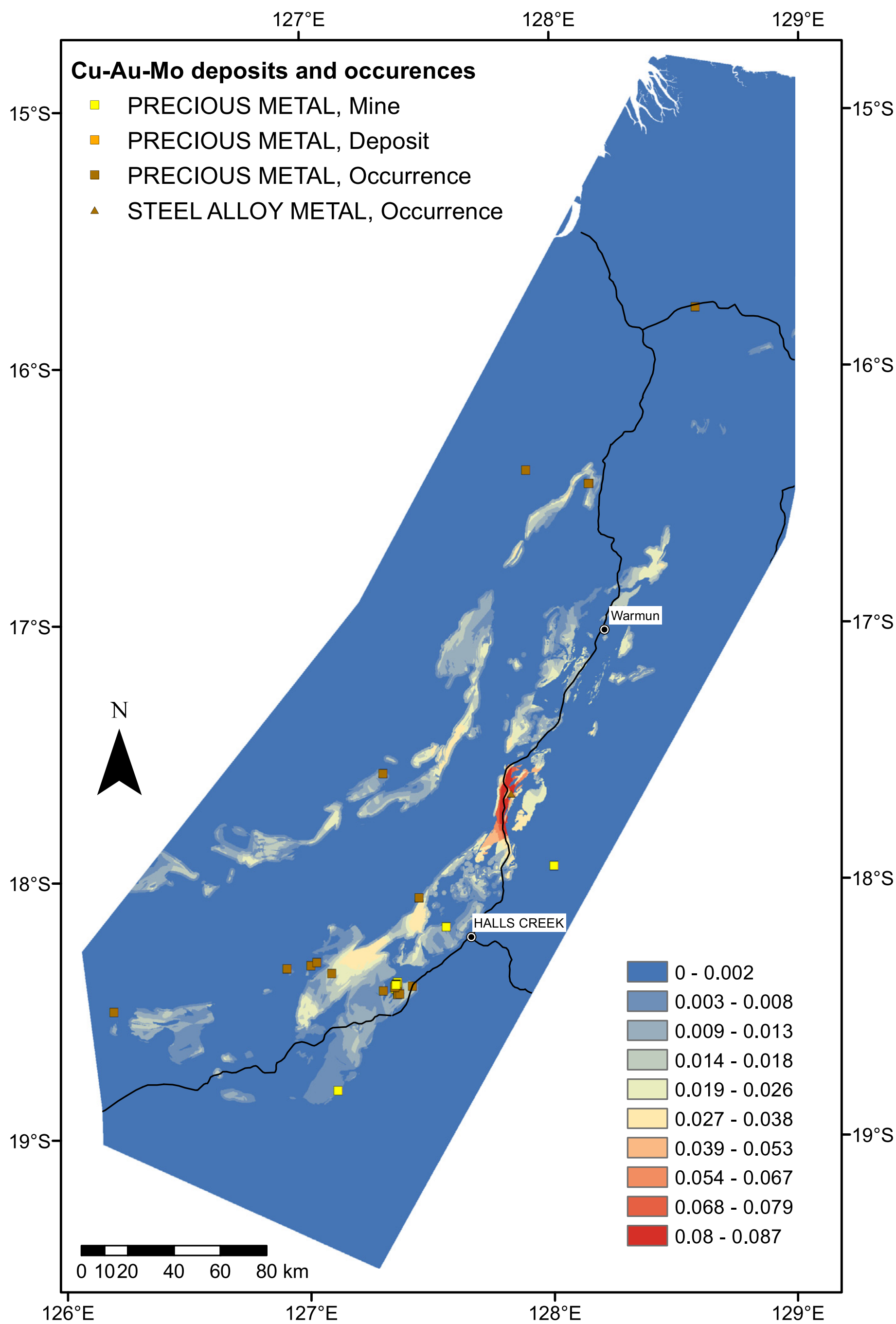

Fig. 15. Prospectivity analysis for Cu, Au, Mo.

pressures between 3.5 and 5 kb towards the end of the Hooper Orogeny, and locally during the early stages of the Halls Creek Orogeny (recorded in mafic to ultramafic rocks), even though peak amphibolite facies metamorphic conditions may have been more widespread (Bodorkos et al., 1999). Bodorkos et al. (2002) suggest that the high temperature, low pressure metamorphic conditions observed in the central part of the Halls Creek Orogen have been induced by asthenospheric upwelling, producing a mantle-related transient thermal anomaly that is concomitant with the earliest mafic–ultramafic intrusions into the region. The asthenospheric upwelling is implied to have been induced by slab breakoff at c. 1860 Ma, during the early Hooper Orogeny (Bodorkos et al., 2002). Some variation in the metamorphic grade along and across the central zone is implied to be related to differential uplift and exhumation.

An elliptical domain of high-grade granulite to upper amphibolite rocks is in sharp contact with rocks metamorphosed at medium grade (amphibolite) during both the Hooper and Halls Creek orogenies (Bodorkos et al., 1999), signifying the presence of faults (perhaps thrust imbricates) separating units of different metamorphic grade. Furthermore the existence of intrusive (Sally Malay ultramafic to mafics) and contemporaneous extrusive rocks (Koongie Park Formation supracrustals) in the Halls Creek region, but in the central to north, and southern part of the Halls Creek Orogen, respectively suggests differential exhumation along the belt.

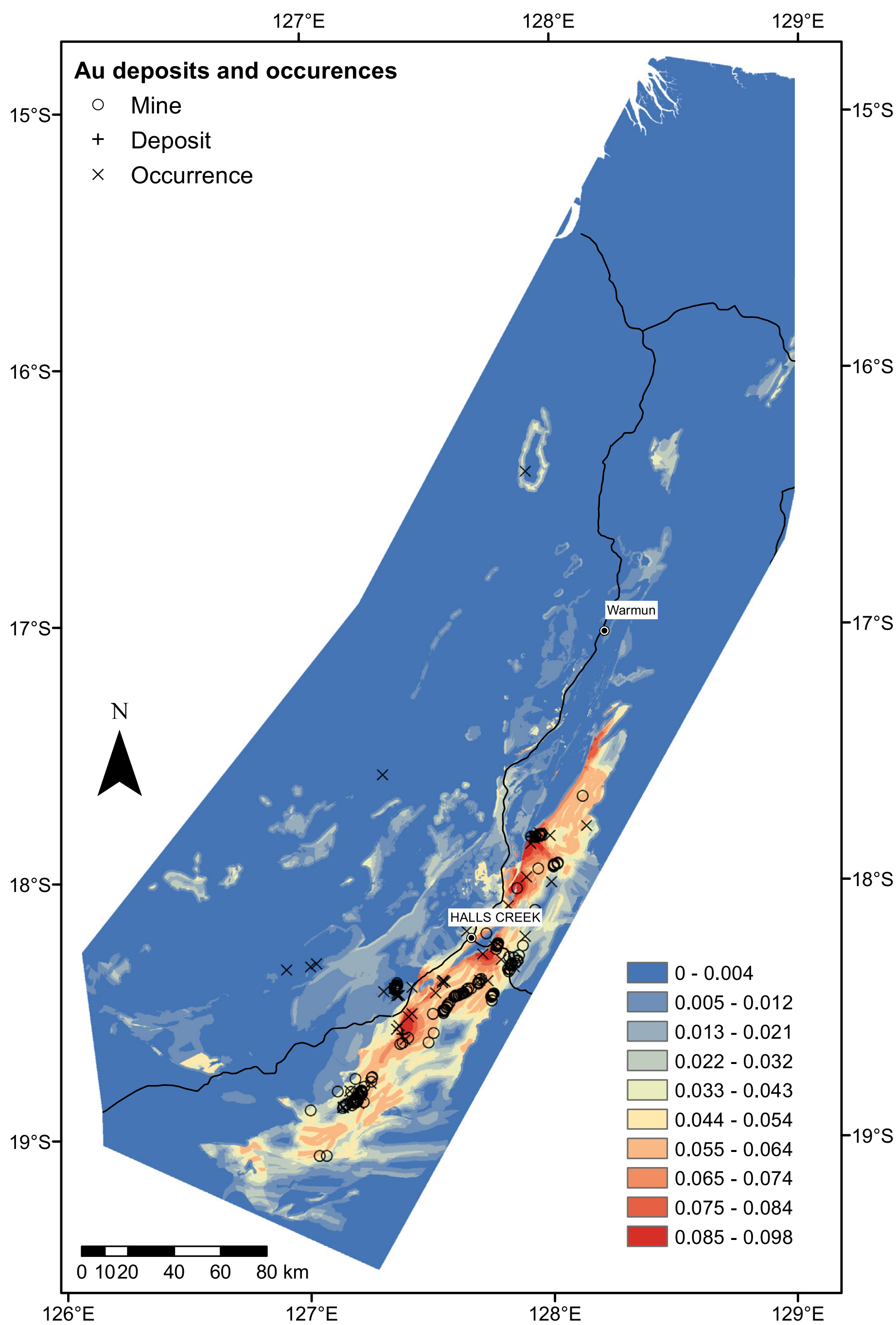

Fig. 16. Prospectivity analysis for Au-only.

3. Prospectivity analysis

3.1. Mineral prospectivity modelling

Seven commodity groups were delineated for mineral systems analysis based on the similarity of key elements required to form and preserve different commodities. Models were derived for each of the groups described.

Mineral prospectivity maps highlight regions that have coincident geological features important for a given commodity, and can play an important role in ensuing regional exploration programmes (Bonham-Carter, 1994; Carranza, 2009). The maps do not directly delineate exploration targets, however they are the results of integrating and overlaying data that can be linked with mineral deposit generation. We chose fuzzy logic, as the knowledge-driven method to perform prospectivity analysis, integrating the previously discussed geological concepts linked to the formation of mineral deposits. Knowledge-driven mineral prospectivity mapping is appropriate in greenfields regions where no, or few, mineral deposits are known. In this regard, the Halls Creek Orogen is considered a greenfields region for all the mineralization types analysed in this study.

3.2. Predictor maps

Fuzzy logic prospectivity models comprise a set of predictor maps representing different components of the mineral system. The predictor maps represent particular geological features of the mineral system that are with certain probability necessary for the mineralization processes

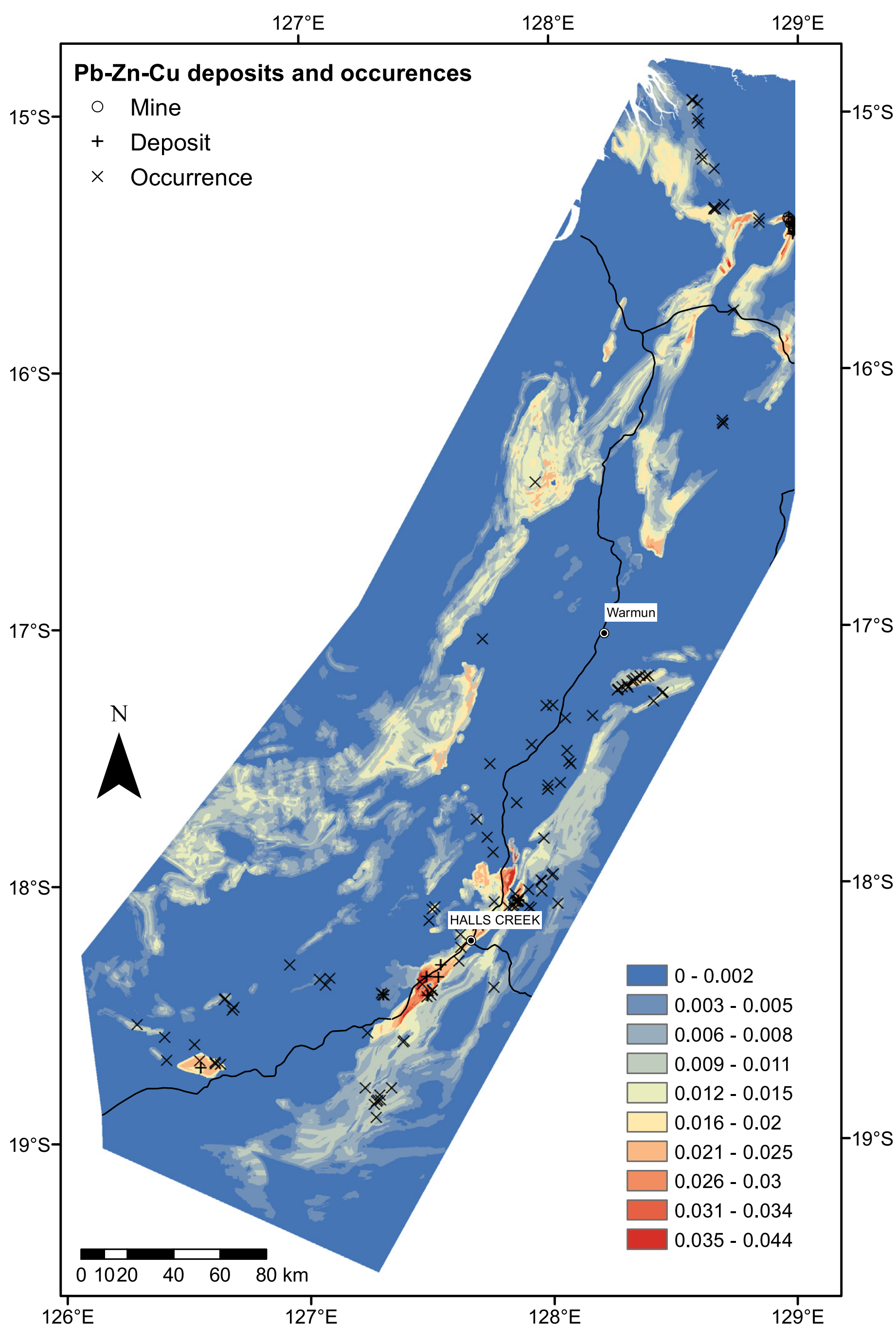

Fig. 17. Prospectivity analysis for Pb, Zn, Cu and Ag.

to occur. The selected fuzzy logic-based inference network models require several predictor maps to be assigned membership values based on a combination of objective datasets and subjective model components. For example, major deep-penetrating faults, acting as pathways for mineralising fluids, can also be the depositional site of mineralisation (Cox et al., 2001). Proxies for fertile zones may be characterized by particular geological units, which have connectivity to the source of metals at depth (e.g. mafic–ultramafic sills). Similarly, a metamorphic map can constitute a proxy for the preservation potential of a mineral system in specific crustal zones. The individual membership values represent cell-by-cell weighting of a predictor map in the mineral system model.

The modelling followed the steps described by Lindsay et al. (2015a, 2015b, 2015c): (1) identification of mappable proxies of key components of a particular mineral system (2) generation of predictor maps based on these proxies (3) assigning map weights, class weights and confidence factors to the predictor maps (4) estimating fuzzy membership values for each predictor map; and (5) generating a prospectivity model through the overlay of weighted predictor maps in a fuzzy inference network (Joly et al., 2012).

All of the predictor map class weights vary between 0.001 and 1 (1 being the most prospective). We have used a linear membership function where w_j corresponds to class weight and x to the numeric value of the class (Eq. (1)).

$$w_j(x) = \begin{cases} 0.001 & x < x_{min} \\ \frac{x - x_{min}}{x_{max} - x_{min}} & x_{min} < x < x_{max} \\ 1 & x > x_{max} \end{cases} \quad (1)$$

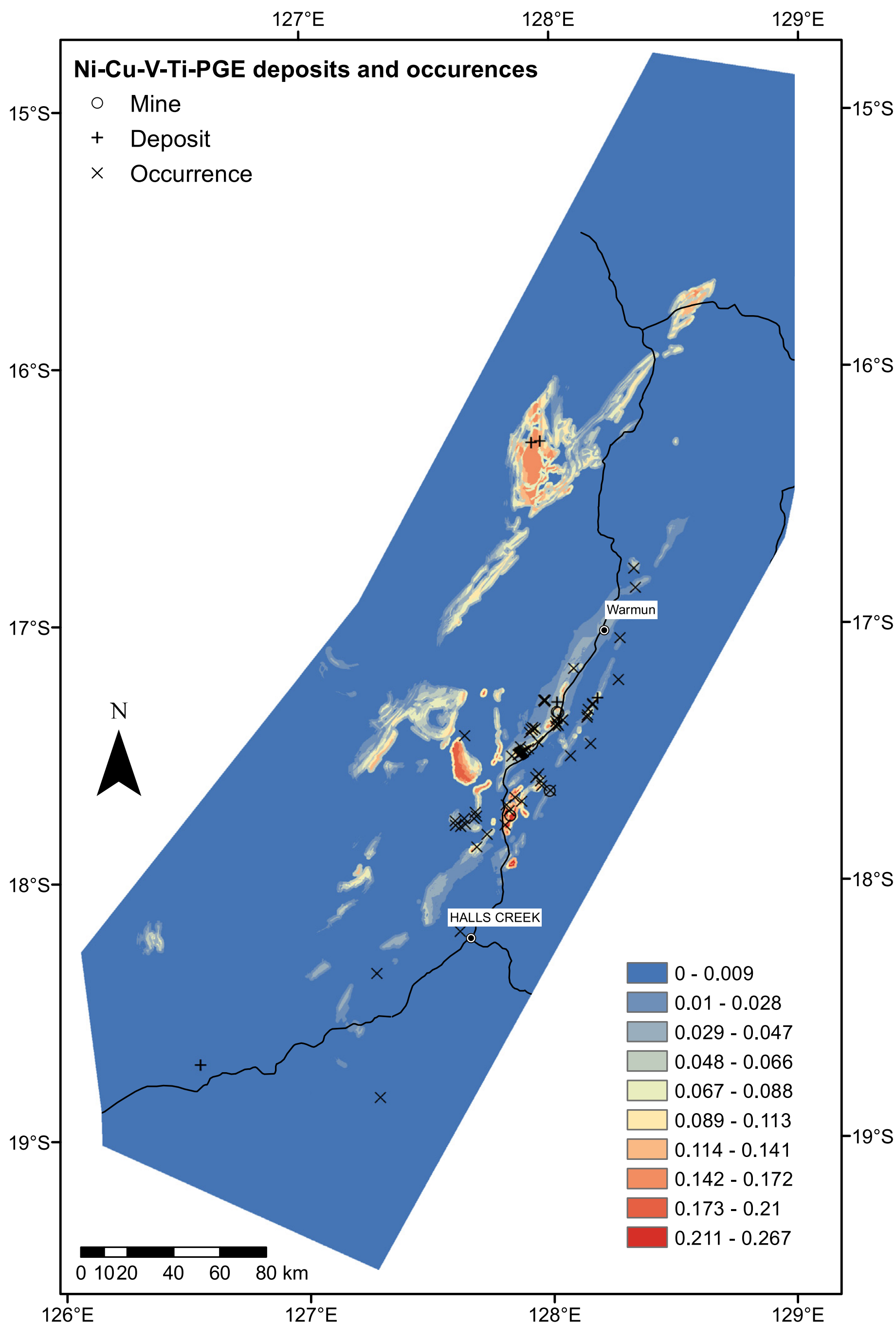

Fig. 18. Prospectivity analysis for Ni–Cu-PGE-V–Ti.

Most of the predictor maps describe the distance to prospective features. For these predictor maps, the class-weights correspond to a decrease in prospectivity with increasing distance to a cut-off value from an object of interest. Zero values were not assigned as some of the fuzzy logic operators used in the inference network would render areas with a zero value component of the mineral system as completely unprospective. Spatial density of features was also used and linearly decreasing classes of the density function were assigned up to a cut-off value. Categorical evidence layers such as metamorphic zones were used with expert determination of class weights according to the relative class importance.

Each value (fuzzy membership) on a predictor map is a product of the map weight, class weight and confidence factor at each point. The overall membership in the fuzzy inference network corresponds to

$$\mu_{\sim A_i} = m_i \times w_j \times cf_i;\ \text{where } m_i \in 0;1; w_j \in 0;1; cf_i \in 0;1. \quad (2)$$

Various 'operators' are available to facilitate the combination of different predictor maps in a fuzzy logic model (Bonham-Carter, 1994). In this study the fuzzy OR, fuzzy algebraic SUM, and fuzzy algebraic PRODUCT were used. The fuzzy operators provide a means for emphasising or moderating certain prospectivity factors (see Joly et al., 2012; Lindsay et al., 2015a, 2015b, 2015c, for more details).

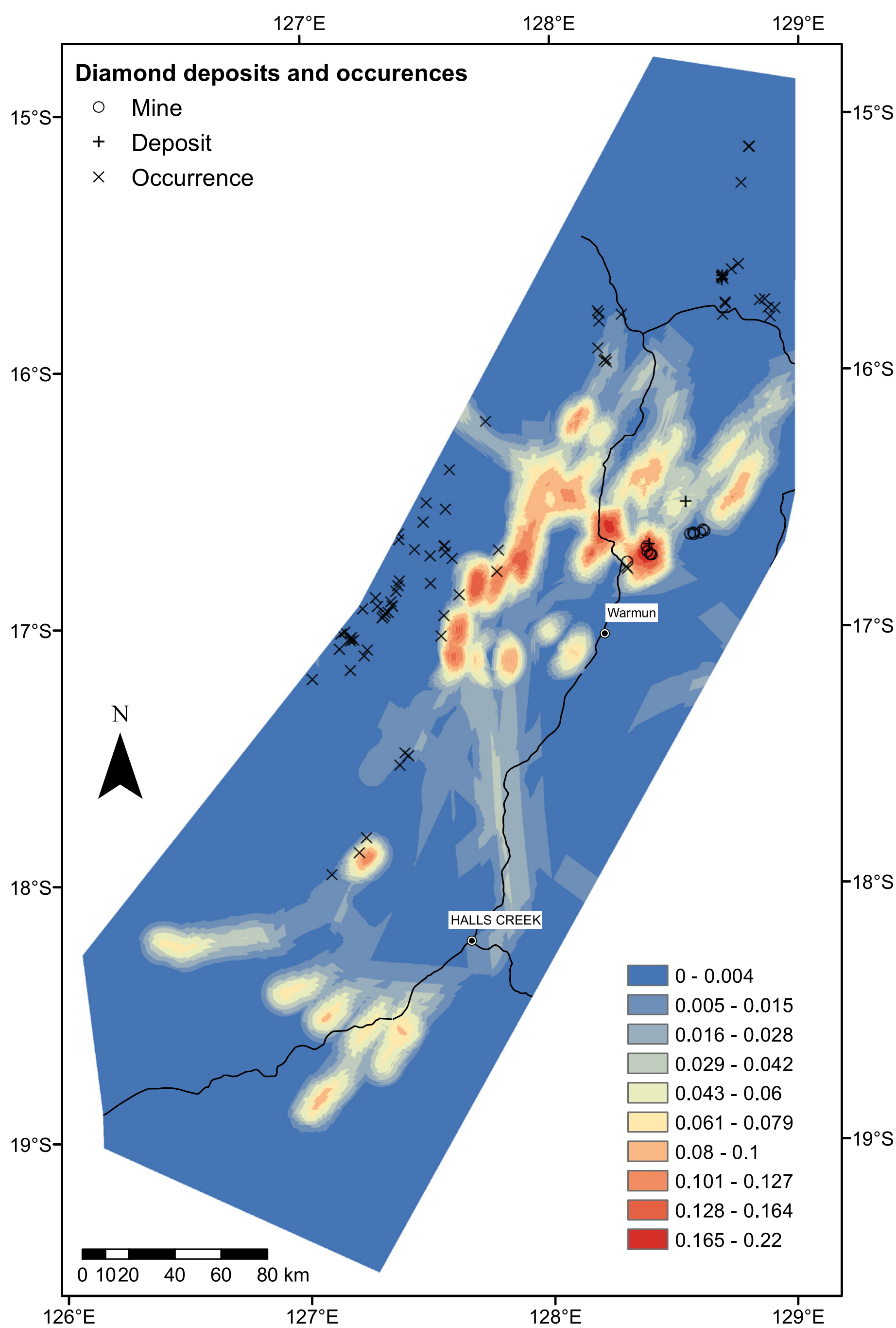

Fig. 19. Prospectivity analysis for diamonds.

Table 4
Search area statistics illustrating prospectivity analyses can vastly reduce the exploration search area.

Mineral system	Percentage of map in top 50% of the range of prospectivity values	Area (km^2)
REE	0.74	26.87
Cu–Au–Mo	0.23	27.47
Diamonds	0.76	29.24
Ni-Cu-PGE-V-Ti	0.51	16.53
Au	3.72	152.7
Sn–W–Mo	4.32	331.1
Pb–Zn	0.75	29.49
	Total area 75,261 km^2	

A 100 m unit cell size was chosen for the predictor maps and the final prospectivity products as best representing the resolution of the geophysical and geological data. A different global map weight, m_i (Eq. (2)) was applied to each branch of the network reflecting its importance — fertility $m_i = 0.9$, crustal architecture $m_i = 0.7$, preservation $m_i = 0.5–0$, geodynamic throttle and deposition site $m_i = 0.5$. Confidence factors cf_i (Eq. (2)) were attributed to each of the predictor maps based on the perceived reliability of the data and their ability to accurately define a particular mineral system component. The perception of reliability is generally low where the data provide an imperfect proxy for the desired mineral system component (Table 2). Table 2 shows the classifications used, the confidence factors and the map weights. It also depicts how the predictor maps were combined in the intermediate steps. The overall overlay operator is a penalty-function

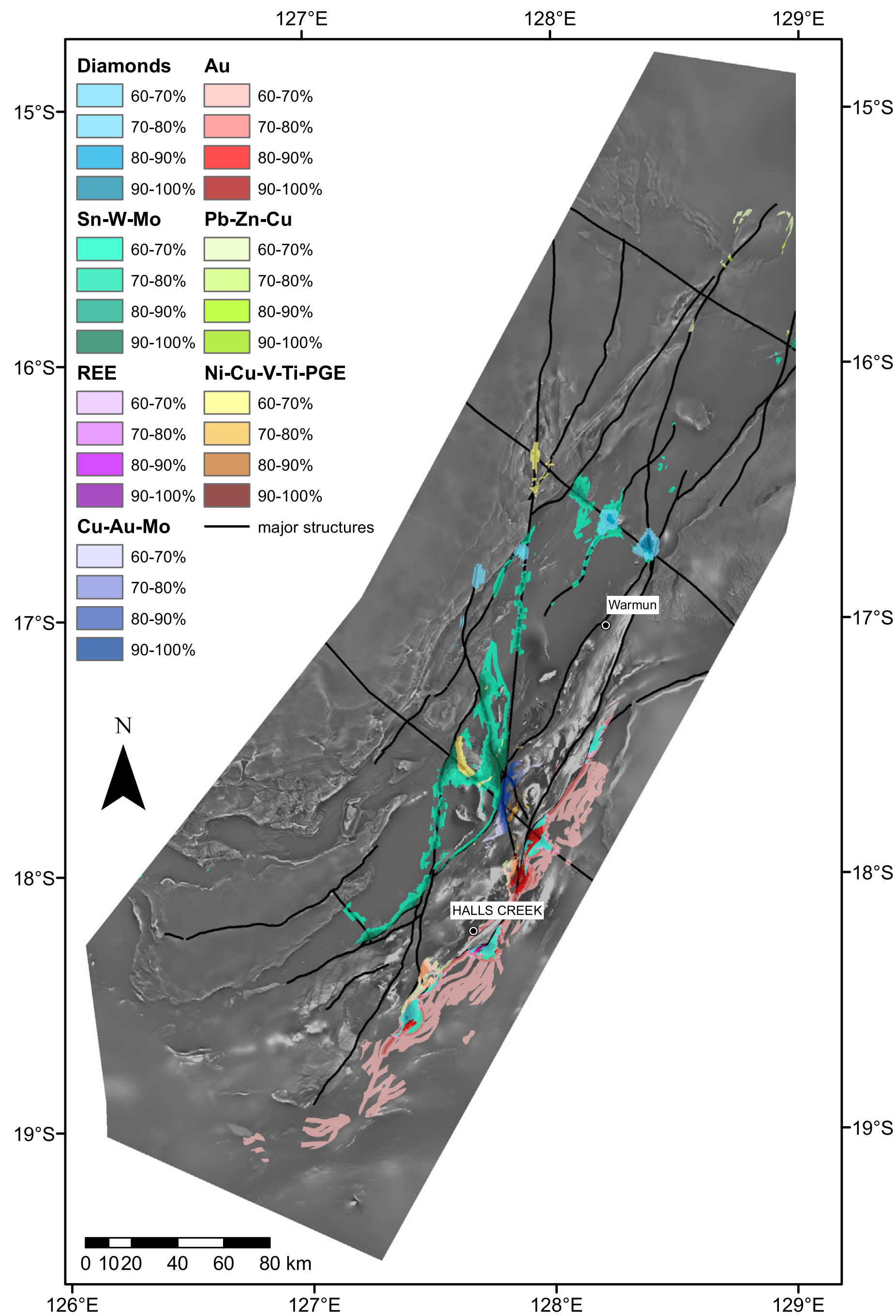

Fig. 20. Map of prospectivity for diamonds, Au, Sn–W–Mo, Pb–Zn–Cu, REE, Ni–Cu–V–Ti-PGE and Cu–Au–Mo in the top 50% percent of the range of prospectivity values.

that returns the product of several fuzzy layers. It penalises pixels with low-fuzzy values, and does not emphasise values from the dominant set. The fuzzy product operator is conservative which is appropriate for a greenfields region with limited mineral deposit data.

3.2.1. Crustal-scale architecture

The average orientation of major lithospheric scale faults was calculated and sub-divided according to their N, NW, or NE trend. The N–S oriented major faults were ascribed highest confidence factor (0.9), while the NW striking orogen normal structures obtained a confidence factor of 0.8. The least confidence (0.7) was given to the NE striking faults, because their existence was less well demonstrated. A 10 km cut-off distance was applied as the limit beyond which the influence of a particular fault was considered negligible. For some models smaller faults were used and the buffer distance decreased to 5 km. The 'distance to faults' layers were weighted by their confidence factors and combined using the fuzzy OR operator. The intersection of major faults was considered particularly prospective and a 10 km buffer was used (Fig. 9). At fault intersections, fluid flux may have been intensified; hence these features were combined with the fuzzy algebraic SUM operator, which had an increasive effect. The distance classes for all of the predictor maps describing the crustal scale architecture corresponded to 1 km intervals.

3.2.2. Geodynamic throttle, depositional site

The geodynamic throttle and depositional parameters of mineral systems were grouped together because the respective predictor maps overlap in many instances. For example, fault bends can also act as favourable depositional zones. The fault bends density map (Fig. 10) was derived as kernel density of point features per km^2 representing major changes in orientation along fault lines. The fault line vertices, corresponding to major changes in fault line orientations, were calculated using a search neighbourhood of 10 km. A class division value of 0.0015 (resulting in 11 classes) was used along with a saturation value of 0.05 above which the maximum membership value of 1 was used. The intersection of non-major faults could represent significant damage zones where metal precipitation may occur. A density map of the intersections per km^2 was calculated using a 10 km search neighbourhood. Eleven classes were used with a class division value of 0.005 and a saturation value 0.05. The final density map, the overall structural complexity was calculated as the kernel density of all line features (lithological boundaries, faults, fold axes, dykes). Here 11 classes were again used with a class division value of 0.2 and saturation value of two. Locations with dense structural framework are regarded as effective traps for mineralisation.

Contacts between lithological units with differing rheological or geochemical reactivity properties are regarded as preferential trap sites (Brown, 2002). The rheological and geochemical contrast maps were created by assigning to each interpreted lithological unit a relative rheology and relative geochemical reactivity value (Fig. 11; Brown, 2002).

Lithological contacts were then assigned a difference value of the respective rheological and geochemical reactivity properties of two adjacent units. Line density per km^2 was computed for contacts with contrast values larger than zero. A search radius of 10 km was applied while the lines were weighted by the corresponding contrast value.

Distance to fold axes was used to indicate fluid trap zones. The identification of fold axes was not straightforward and probably resulted in an incomplete dataset, which caused in a lower confidence value of this predictor map. The classes correspond to 1 km distance zones up to a buffer value of 5 km beyond which the influence is considered negligible.

For the Sn–W prospectivity model a distance to the 2.5% K content boundary was used as predictor map as spatial correlations were observed to mineral occurrences along this threshold. Six classes were created with 1 km intervals and a 5 km cut-off/buffer limit.

A Moho depth model was used as proxy to diamond depositional sites, as it is widely accepted that diamond bearing kimberlite pipes occur in zones of thick crust (Aitken et al., 2013). Classes (zones) divided by 5 km in depth were created. The highest membership value was assigned to the deepest zones. Regional zones of the Halls Creek Orogen considered more prospective for diamond occurrences due to their thicker lithosphere (Central and Western Zone, Hart Dolerite, Speewah Group) were also used as proxies. A larger 15 km wide buffer zone was used around these zones to account for the uncertainty in their actual borders.

3.2.3. Fertility

The origin of metals and fluids is connected with specific rock types and forms an important predictor layer in all prospectivity analyses (Fig. 12). The fertility parameter in this study was tied to the presence of selected lithological units, largely as proxies to units within deep source regions which can't be mapped directly. The lithological units were derived from an updated geological map of the area where existing GSWA maps of different scales were combined into a harmonized dataset. Except for the diamond model, a buffer zone of 1 km was used to represent the uncertainty in the exact location of lithological boundaries. A buffer distance of 15 km was utilized around the mapped lamproites and kimberlites occurrences for the diamond model.

Confidence factors were assigned to different lithologies reflecting their perceived ability to act as either fluid or metal sources within a particular mineral system. For diamonds, fertility was also derived from interpreted deep lithospheric architecture shown in the AuSREM model (Kennett et al., 2013). Boundaries where high lateral gradients existed in the vertically polarised shear-wave model were derived during the interpretation. A kernel density function was used to map the complexity of the lithospheric boundaries in the study area. Eleven classes were used with a class division value of 0.05 and a saturation value of 0.45. The fertility predictor maps were combined using the fuzzy OR operator so that the maximum value of each predictor map was retained in the inference network.

3.2.4. Preservation

The preservation component may be important for certain mineral systems such as gold and copper–gold, but not as important for the Ni–Cu–Ti–V–PGE systems which are known from greenschist to the granulite facies (Fig. 3). The metamorphic map (Fig. 6) created during this study was used as proxy for the preservation component of mineral systems. Different expert classifications were used for different commodity groups (see Table 3). The higher the number assigned, the higher the fuzzy membership of the class in the model.

The preservation component was not used at all for the diamond model or the Ni, Cu, Ti, V, PGE model. A lower map weight of 0.3 was used in the Pb, Zn, Cu model because the metamorphic grade is regarded less important for the preservation of these mineral deposits, e.g. the high grade Broken Hill Pb–Zn deposit (Leach et al., 2010).

4. Results

Deep crustal-scale structures are critical to the formation and deposition of minerals assigned to all the commodity groups targeted in this exercise. For some prospectivity models rock type as a proxy for fertility or depositional site was considered to be important and were thus weighted heavily, and therefore highly influential on the resulting prospectivity map.

Prospectivity mapping for areas most likely to be fertile in tin (Sn) and tungsten (W) focussed on areas containing granitoid rocks that formed in either an intraplate setting, or distal from a subduction zone (Paperbark Supersuite), or in areas associated with pegmatite or veins of quartz, quartz-carbonate, quartz-tourmaline that have intruded late in the Halls Creek Orogeny (Sanders, 1999). Individual pegmatite veins, or small granite stocks were not captured during this regional-scale analysis, so were not included. Molybdenum (Mo), was also considered in this group, mainly because it is associated with Sn and Win the database for the region. Through this analysis, it was found that the eastern zone, particularly in the south, and regions in the western zone where deep crustal-scale structures intersect granite of the Paperbark Supersuite may be most prospective for Sn, W and Mo mineralisation (Fig. 13)

Mineral occurrences of REE are mainly limited to the eastern zone, apart from one occurrence reported in the central part of the central zone, where it is associated with a carbonatite (copperhead occurrence, minedex database, Z52 377571E, 8041059N). The single occurrence in the central zone is in a region that contains several intersecting deep crustal-scale faults mapped from gravity and magnetic data (Lindsay et al., 2015b), and the Cummins Range carbonatite complex in the eastern zone is also associated with large-scale faults (Downes et al., 2014).

Targeting for REE at a regional-scale is problematic, as is illustrated by the failure to capture the occurrences in the southeastern most part of the study area in the Cummins Range. The number of appropriate evidence layers for this analysis was insufficient, or too low resolution to place much importance on the results. This is compounded because REE occurrences are often associated small stocks of alkaline intrusive rocks or carbonatites (London, 2011), which were not represented on the regional-scale maps we used in the analysis. Despite this, in the central zone an area mapped as Syenite Camp Suite was considered a proxy for a possible source region (at depth) for REE occurrences, mainly due to its proximity to the Copperhead occurrence and association with intersecting north, northeast and northwest trending fault zones (Fig. 14). The analysis through this zone supports that REE most likely occur proximal to major faults (Downes et al., 2014), suggesting that they may extend into the western zone in areas of high structural complexity (e.g. around Speewah Dome).

Specific areas within the western, central and eastern zones were all found to be prospective for Cu–Au–Mo. However, the most prospective zone delineated through this analysis was in the, middle part of the central zone in the Syenite Camp Granite, where it lies over major deep crustal scale structures and is not considered to have undergone significant metamorphism (Fig. 15). Even though this region is considered prospective for Cu–Au–Mo mineralisation that may be associated with porphyry-style deposits, porphyry style mineralisation over this zone has not been reported, nor have igneous rocks that form in the roof zones of granitic intrusions been described. The analysis may have highlighted a deep feeder zone to a porphyry system that has been exhumed and eroded. Currently the sensitivity of the preservation component of the analysis is not sufficiently constrained to highlight differences in the upper few kilometres of the crust.

A gold-only (Au) prospectivity analysis was completed in the region taking into account preservation level (using the proxy of metamorphic grade), rock type, fertility (areas that are considered to have developed above a subduction zone), connectivity to deep crustal scale structures, complexity of structure, possible dilation zones and jogs in the dominant structural grain of the region, and possible alteration zones (K-metasomatism). For this analysis the formation and deposition of the Au is implied to have occurred during plate convergence, most likely during the Halls Creek Orogeny.

The most prospective regions for Au-only mineralisation were found to be in the eastern zone and some easternmost parts of the central zone (Fig. 16). Complexly deformed parts of the central zone were not considered to be prospective for Au mineralisation because they were metamorphosed at high grade during both the Hooper and Halls Creek orogenies.

In the central zone the Syenite Camp Suite that is located adjacent to three deep crustal scale structures may be prospective. However, this region appears as one of low Au-only prospectivity in the central portion of the map, because the Syenite Camp Suite is not considered to be metamorphosed, even at low grade, which is one of the criterion required for the gold only analysis. Greenschist facies rocks of the Koongie Park Formation are considered to be prospective for Au mineralisation, in zones of high structural complexity. In the eastern zone parts of the Biscay and Olympio Formations that are in areas of high structural complexity or around fault jogs are considered the most prospective. The only area in the western zone that may be prospective for Au mineralisation was found to be around the Speewah Dome, above the northerly trending deep crustal scale structure. For this analyses all reported Au deposits and mines were captured (validated by GSWA datasets; Fig. 16).

Areas known for small deposits or mining for base metals (including variable amounts of lead zinc or copper) occur in the southern part of the central zone within the Paleoproterozoic Koongie Park Formation, in the northernmost extent of the area analysed in Devonian limestone reef complexes of the Ningbing Group preserved on the northwest trending Ningbing horst block, and Carboniferous carbonates of the Bonaparte basin that developed around the flanks of the Proterozoic Pincombe Inlier (Fig. 17). Occurrences of Devonian and Carboniferous Pb–Zn deposits are reportedly stratabound, forming in Mississippi-valley type deposits, whereas the Cu–Pb–Zn–Ag occurrences and deposits in the Koongie Park Formation formed in as volcanogenic massive sulphides (Sanders, 1999; Sewell, 1999).

The prospectivity analysis outlined that areas of volcanosedimentary rocks of the Koongie Park Formation that are adjacent to deep crustal scale structures are most prospective for Pb–Zn–Cu–Ag deposits, particularly adjacent to the central-eastern zone boundary, and in the southern part of the central zone. In addition to this, all regions containing outcropping, or regolith covered occurrences of Devonian and Carboniferous carbonates, particular adjacent to large scale faults and basement highs are prospective for Pb and Zn. One region of interest includes an ENE trending part of the Paleo to Neoproterozoic Bungle Bungle Dolomite in the central part of the eastern region of the study area which was found to be slightly prospective for Pb–Zn.

In the southwestern part of the study area, the Bohemia zinc and Black Spur group of Pb–Zn prospects occur in Devonian carbonate rocks that underlie the siliciclastic Permian Grant Group. These prospects were not found in the prospectivity analysis, due to the analysis being completed in 2D, with no reference to the Devonian carbonate sequences underlying the Grant Group.

Parts of the Speewah Group in a triangular zone between northwest, north and northeast trending major crustal scale structures was found to be slightly prospective for base metal style commodities. In this region the high fault density, intersection of major structures could highlight the possible potential for base metal occurrences; however, none have been reported. The Tickalara Metamorphics in the central zone was not found to be prospective in this analysis even though there are reported occurrences of base metals from this unit. This is because the regional-scale resolution used for the analysis is too low to capture any prospectivity within individual rock types of the Tickalara Metamorphics.

The main influences on the prospectivity analysis for nickel (Ni), copper (Cu), platinum, palladium and gold (PGEs), vanadium (V), and titanium (Ti) in this analysis was the assumption that mafic to ultramafic rocks are a proxy for fertility for the formation or, and suitable depositional site for these (mafic to ultramafic rocks). Additionally, proximity to orogen normal or northerly trending deep crustal scale faults was considered favourable. In the analysis, areas where ultramafic to mafic rocks lie over orogen-perpendicular faults that cut the Halls Creek Orogen, or the large-scale northerly trending fault that cuts through the central and western zones were found to be most prospective for Ni, Cu, PGE's, Ti and V, and both coincident with mineral deposits and occurrences already known in the region and highlight areas where mineral deposits have not been documented. As the deposition of these commodities in the crust is independent of the level of crustal exposure features such as metamorphic grade do not influence the analysis (Figs. 6 and 18).

Most diamond occurrences in the east Kimberley region are alluvial diamonds, in which the source of the causative alkaline intrusive is apparently unknown. For this analysis a depth to Moho map was used to indicate very deep crustal scale structures and lithospheric thickness, interpreted by analysing rapid changes in lithospheric thickness across the Halls Creek Orogen. The resulting prospectivity maps illustrates that diamonds are most likely to have been deposited in the central or eastern zones, along deep crustal scale structures (preferably NW or N trending) (Fig. 19). In the southern Halls Creek Orogen, within the central zone a NW trending zone of possible diamond prospectivity is delineated, where no known alkaline intrusives have been reported.

4.1. Search space reduction

Prospectivity mapping is an effective tool in communicating complex interactions between a variety of different geoscientific datasets. The value to explorers from prospectivity maps is the reduction of geographical search space, making ground selection a faster and more rigorous process. We display the efficacy of this study in reducing the geographical search space quantitatively (Table 4) and spatially (Fig. 20). Table 4 shows that the exploration search space for most commodity groups could be narrowed down to less than 0.04% of the total area, except for Au and Sn–W–Mo for which the analysis narrows the search space down to less than 0.5%. In geographic terms this reduces the area of ground to be analysed at camp scale to less than 620 km^2 for all commodities reviewed in this study (Fig. 20). Fig. 20 shows that for the western, central and eastern zones the most highly prospective areas are proximal to deep crustal-scale structures, above which there is some, but not pronounced overlap of prospectivity of different commodity groups.

5. Conclusions

This study sought to develop models to characterise areas of mineral prospectivity for a group of seven commodities or mineral types of various ages and ore genesis mechanisms.

The work clarifies the extents of major structures and links the interpretation of Lindsay et al. (2015b) and mineral system analysis to the structural and tectonic history of the region.

The work illustrates that crustal-scale tectonic architecture can be analysed by allying the geological-geophysical interpretation with 2.5D magnetic and gravity modelling, from which ore deposition mechanisms can be inferred, and therefore prospectivity. Through this we show different tectonic ‘zones’ of the Halls Creek Orogen are prospective for diverse commodity groups (Fig. 20). We include in this analysis: the tectonic environment in which commodities may have developed in through time; the relative preservation zones conserved at the surface or subsurface; and favourable depositional sites that may be present in these zones (structural, or lithological).

Major crustal-scale faults or shear zones identified by Lindsay et al. (submitted) are shown to control the location of ore deposits already known from the area, and are therefore implied to be sites of fluid migration, and overlying or proximal to them sites of ore deposition. Of these orogen-perpendicular (northwest trending) and orogen-oblique (north trending) faults seem to be the most influential structures with respect to ore deposition in the Halls Creek Orogen, especially where they intersect each other or orogen-parallel faults and shears.

In summary, the eastern zone appears to be the most prospective for Au-only mineralisation, whereas the central zone is perhaps most prospective for Cu–Au–Mo, and Pb–Zn–Cu–Ag mineralisation. Regional-scale prospectivity analysis for REE was difficult to complete mainly due to the resolution of the data used for the analysis, and the relatively small size expected for a REE deposit. In-situ diamond prospectivity might be restricted to the central and western zones, and Cu–Au–Mo mainly in the central zone. The central zone was also found to be prospective for Ni–Cu-PGE's-V–Ti, as were parts of the western zone which along with the eastern zone may be prospective for Sn, W (and Mo) mineralisation.

Acknowledgements

This work was supported by the Geological Survey of Western Australia under the Exploration Incentive Scheme, Royalties for Regions. Ian Tyler publishes with the permission of the Executive Director of the Geological Survey of Western Australia. Our work in the east Kimberley has benefitted from fruitful discussion with many working in the region. In particular we would like to thank: Ken Rogers (King River Copper Pty Ltd); John Hicks and Andrew Shaw-Stuart (Panoramic Resources); Karin Orth (University of Tasmania); David Maidment and Trevor Beardsmore, Sidi Morin-Ka, John Brett and David Twist (GSWA). We also thank the manuscript reviewers Aurore Joly and Walter Witt, who greatly improved it.

References

Aitken, A.R.A., Salmon, M., Kennett, B.L.N., 2013. Australia's Moho: a test of the usefulness of gravity modelling for the determination of Moho depth. Tectonophysics 609, 468–479.

Andrew, B., Eves, A., Ramsey, R., 2012. Speewah Dome Project, Co-funded Drilling Report for the Period Ending 30/06/2012, E80/2863, 3657, and M80/269. Speewah Mining Pty Ltd.

Arndt, N.T., Lesher, C.M., Czamanske, G.K., 2005. Mantle-derived magmas and magmatic Ni-Cu-(PGE) deposits, Economic Geology 100th Anniversary Volume. pp. 5–24.

Begg, G.C., Griffin, W.L., Natapov, L.M., O'Reilly, S.Y., Grand, S.P., O'Neill, C.J., Hronsky, J.M.A., Poudjom Djomani, Y., Swain, C.J., Deen, T., Bowden, P., 2009. The lithospheric architecture of Africa: seimsmic tomography, mantle petrology, and tectonic evolution. Geosphere 5, 23–50.

Begg, G.C., Hronksy, J.A.M., Arndt, N.T., Griffin, W.L., O'Reilly, S.Y., Hayward, N., 2010. Lithospheric, cratonic, and geodynamic setting of Ni–C-PGE sulfide deposits. Econ. Geol. 105, 1057–1070.

Bierlein, F.P., Groves, D.I., Goldfarb, R.J., Dubé, B., 2006. Lithospheric controls on the formation of provinces hosting giant orogenic gold deposits. Mineral. Deposita 40 (8), 874–886.

Blake, D.H., Tyler, I.M., Page, R.W., 2000. Regional geology of the Halls Creek Orogen. In: Hoatson, D.M. (Ed.), Geology and Economic Potential of the Palaeoproterozoic Layered Mafic–Ultramafic Intrusions in the East Kimberley, Western Australia. Australian Geological Survey Organisation, Canberra, pp. 35–62.

Blake, D.H., Tyler, I.M., Griffin, T.J., Sheppard, S., Thorne, A.M., Warren, R.G., 1999. Geology of the Halls Creek 1:100 000 Sheet area (4461). Australian Geological Survey Organisation, Western Australia.

Bodorkos, S., Reddy, S.M., 2004. Proterozoic cooling and exhumation of the northern central Halls Creek Orogen, Western Australia: constraints from a reconnaissance 40Ar/39Ar study. Aust. J. Earth Sci. 51 (4), 591–609.

Bodorkos, S., Oliver, N.H.S., Cawood, P.A., 1999. Thermal evolution of the central Halls Creek Orogen, northern Australia. Aust. J. Earth Sci. 46, 453–465.

Bodorkos, S., Sandiford, M., Oliver, N.H.S., Cawood, P.A., 2002. High-T, low-P metamorphism in the Palaeoproterozoic Halls Creek Orogen, northern Australia: the middle crustal response to a mantle-related transient thermal pulse. J. Metamorph. Geol. 20, 217–237.

Bonham-Carter, G.F., 1994. Geographic information systems for geoscientists: modeling with GIS. Computer Methods in the Geosciences 13. Elsevier.

Brown, W., 2002. Artificial Neural Networks: A new Method for Mineral-prospectivity Mapping (Doctor of Philosophy Thesis), University of Western Australia, Perth (441 pp.).

Carranza, E.J.M., 2009. Geochemical Anomaly and Mineral Prospectivity Mapping in GIS 11. Elsevier.

Cawood, P.A., Hawkesworth, C.J., 2013. Temporal relations between mineral deposits and global tectonic cycles. In: Jenkins, G.R.T., Lusty, P.A.J., McDonald, I., Smith, M.P., Boce, A.J., Wilkinson, J.J. (Eds.), Ore Deposits in an Evolving Earth. Geological Society, London, Special Publication, London (http://sp.lyellcollection.org/content/early/2013/10/18/SP393.1).

Cawthorn, R.G., 1996. Layered Intrusions. Elsevior 531p.

Cline, J.S., Hofstra, A.H., Muntean, J.L., Tosdal, R.M., Kickey, K.A., 2005. Carlin-type gold deposits in Nevada: critical geologic characteristics and viable models. In: Hedenquist, J.W., Thompson, J.F.H., Goldfarb, R.J., Richards, J.P. (Eds.), Society of Economic Geolgists Special Publication, pp. 451–484.

Cox, S.F., Knackstedt, M.A., Braun, J., 2001. Principles of structural control on permeability and fluid flow in hydrothermal systems. Soc. Econ. Geol. Rev. 14 (1), 1–24.

D'Ercole, C., Groves, D.I., Knox-Robinson, C.M., 2000. Using fuzzy logic in a Geographic Information System environment to enhance conceptually based prospectivity analysis of Mississippi Valley-type mineralisation. Aust. J. Earth Sci. 47 (5), 913–927.

Dorling, S.L., Dentith, M.C., Groves, D.I., Vearncome, J.R., 1996. Mississippi Valley-type deposits of the Southeastern Lennard Shelf: an example of the interplay of extensional deformation, sedimentation and mineralization. In: Sangster, D.F. (Ed.), Carbonate-hosted lead-zinc deposits. Society of Economic Geologists, pp. 96–111.

Downes, P.J., Demeny, A., Czuppon, G., Jaques, A.L., Verrall, M., Sweetapple, M., Adams, D., McNaughton, N.J., Gwalan, L.G., Griffin, B.J., 2014. Stable H–C–O isotope and trace

element geochemistry of the Cummins Range Carbonatite Complex, Kimberley region, Westerns Australia: implications for hydrothermal REE mineralization, carbonatite evolution and mantle source regions. 49, 905–932.
Ferguson, K.M., 1999. Lead, zinc and silver deposits of Western Australia. In: G.S.o.W. Australia (Ed.), Mineral Resources, Bulletin 15 (314 pp.).
Fiorentini, M.L., 2007. Prospectivity of the Hart Dolerite, Halls Creek Orogen, North Kimberley, Western Australia. In: Smith, G. (Ed.), E80/3277, E80/3278, E80/3445, E80/3446, E80/3448 Relinquishment Report, Elemental Minerals. GSWA Open File Mineral Exploration Report a076531.
Fishwick, S., Kennett, B.N.L., Reading, A.M., 2005. Contrasts in lithospheric structure within the Australian Craton — insights from surface wave tomography. Earth Planet. Sci. Lett. 231, 163–176.
Garwin, S., Hall, R., Watanabe, Y., 2005. Tectonic setting, geology, and gold and copper mineralization in Cenozoic Magmatic Arcs of Southeast Asia and the West Pacific. In: Hedenquist, J.W., Thompson, J.F.H., Goldfar, R.J., Richards, J.P. (Eds.), Economic Geology, One Hundredth Anniversary Volume, 1905–2005. Society of Economic Geologists, Inc., Littleton, Colorado, pp. 891–930.
Goldfarb, R.J., Groves, D.I., Gardoll, S., 2001. Orogenic gold and geologic time: a global synthesis. Ore Geol. Rev. 18, 1–75.
Gorczyk, W., Hobbs, B., Gessner, K., Gerya, T., 2013. Intracratonic geodynamics. Gondwana Res. 24, 838–848.
Grauch, V.J.S., Rodriguez, B.D., Bankey, V., Wooden, J.L., 2003. Evidence for a Battle Mountain-Eureka crustal fault zone, north-central Nevada, and its relation to Neoproterozoic-Early Paleozoic continental breakup. J. Geophys. Res. Solid Earth 108 (B3).
Griffin, T.J., Tyler, I.M., Playford, P.E., 1993. Explanatory Notes on the Lennard River 1:250 000 Geological Sheet SE/51-8, Western Australia. 3rd edition. Geological Survey of Western Australia.
Griffin, T.J., Page, R.W., Sheppard, S., Tyler, I.M., 2000. Tectonic implications of Palaeoproterozoic post-collisional, high-K felsic igneous rocks from the Kimberley region of northwestern Australia. Precambrian Res. 101 (1), 1–23.
Groves, D.I., Bierlein, F.P., 2007. Geodynamic settings of mineral deposit systems. J. Geol. Soc. Lond. 164, 19–30.
Groves, D.I., Bierlein, F.P., Meinerty, L.D., Hitzman, M.W., 2010. Iron oxide copper–gold (IOCG) deposits through earth history: implications for origin, lithospheric setting, and distinction from other epigenetic iron oxide deposits. Econ. Geol. 105, 641–654.
Gurney, J.J., Helmstaedt, H.H., Le Roex, A.P., Nowicki, T.E., Richardson, S.H., Westerlund, K.J., 2005. Diamonds: crustal distribution and formation processes in time and space and an integrated deposit model. In: Hedenquist, J.W., Thompson, J.F.H., Goldfarb, R.J., Richards, J.P. (Eds.), Economic Geology 100th Anniversary Volume. Society of Economic Geologists, pp. 143–177.
Gurney, J.J., Helmstaedt, H.H., Richardson, S.H., Shirley, S.B., 2010. Diamonds through time. Econ. Geol. 105, 689–712.
Hassan, L.Y., 2004. Mineral occurrences and exploration potential of the West Kimberley. Report 88.
Hayward, N., Skirrow, R.G., 2010. Geodynamic setting and controls on iron oxide Cu–Au (+/−U) ore in the Gawler Craton, South Australia. In: Porter, T.M. (Ed.), Hydrothermal Iron Oxide Copper–Gold and Related Deposits: A Global Perspective, pp. 119–145.
Hoatson, D., 2000. Geological setting, petrography, and geochemistry of the mafic–ultramafic intrusions. In: Hoatson, D.M. (Ed.), Geology and Economic Potential of the Palaeoproterozoic Layered Mafic–Ultramafic Intrusions in the East Kimberley, Western Australia. Australian Geological Survey Organisation, Canberra, pp. 99–162.
Hoatson, D., Blake, D.H., 2000. Geology and economic potential of the Palaeoproterozoic layered mafic–ultramafic intrusions in the East Kimberley. Western Australia, Bulletin 246. Australian Geological Survey Organisation, Canberra.
Hoatson, D.M., Lewis, B. (Eds.), 2014. Platinum-group Elements in Australia: Geological Setting, Mineral Systems, and Potential. Record 2014/51. Geoscience Australia, Canberra.
Hollis, J., Kemp, A., Tyler, I., Kirkland, C., Wingate, M., Phillips, C., Sheppard, S., Belousova, E., Greau, Y., 2014. Basin formation by orogenic collapse: zircon U–Pb–Hf isotope evidence from the Kimberley and Speewah Groups, northern Australia. Geological Survey of Western Australia, Report, p. 137.
Huston, D., Stevens, B., Southgate, P.N., Muhling, P., Wyborn, L., 2006. Australian Zn–Pb–Ag ore-formation systems: a review and analysis. Econ. Geol. 101, 1117–1157.
Huston, D., Blewett, R.S., Champion, D.C., 2012. Australia through time: a summary of its tectonic and metallogenic evolution. Episodes 35 (1), 23–43.
Jaques, A.L., Milligan, P.R., 2004. Patterns and controls onthe distribution of diamondiferous intrusions in Australia. Lithos 77, 783–802.
Jaques, A.L., Lewis, J.D., Smith, C.B., 1986. The kimberlites and lamproites of Western Australia. In: W.A.G. Survey (Ed.), Bulletin 132 (268 pp.).
Jaques, A.L., O'Neill, H.S.C., Smith, C.B., Moon, J., Chappell, B.W., 1990. Diamondifereous peridotite xenoliths from the Argyle (AK1) lamproite pipe, Western Australia. Contrib. Mineral. Petrol. 104, 225–276.
Joly, A., Powal, A., Mc Cuaig, C.T., 2012. Exploration targeting for orogenic gold deposits in the Granites–Tanami Orogen: mineral system analysis, targeting model and prospectivity analysis. Ore Geol. Rev. 48, 349–383.
Kennett, B.L.N., Fichtner, A., Fishwick, S., Yoshizawa, K., 2013. Australian seismological reference model (AuSREM): mantle component. Geophys. J. Int. 192 (2), 871–887.
Leach, D.L., Sangster, D.F., Kelley, K.D., Large, R.R., Garven, G., Allen, C.R., Gutzmer, J., Walters, S., 2005. Sediment-hosted lead–zinc deposits: a global perspective. Economic Geology 100th Anniversary Volume, pp. 567–607.
Leach, D.L., Bradley, D.C., Huston, D., Pisarevsky, S.A., Taylor, R.D., Gardoll, S.J., 2010. Sediment-hosted lead–zinc deposits in Earth History. Econ. Geol. 105, 593–625.
Leach, D.L., Song, Y., Hou, Z., Yang, T., Xue, C., 2013. The Giant Jinding Zn–Pb deposit: ore formation in an evaporite dome, Lanping Basin, Yunan, China. In: t.S.B. Meeting (Ed.), Mineral deposit research for a high-tech world. SGA, Uppsala, Sweden.
Leader, L.D., Wilson, C.J.L., Robinson, J.A., 2013. Structural constraints and numerical simulation of strain localization in the Bendigo Goldfield, Victoria, Australia. Econ. Geol. 108, 279–307.
Li, X.C., S.V., B., Collins, A.S., Davidson, A., De Waele, B., Ernst, R.E., Fitzsimons, I.C.W., Fuck, R.A., Gladkochub, D.P., Jacobs, J., Karlstrom, K.E., Lu, S., Natopov, L.M., Pease, V., Pisarevsky, S.A., Thrane, K., Vernikovsky, V., 2008. Assembly, configuration, and break-up history of Rodinia: a synthesis. Precambrian Res. 160, 179–210.
Lindsay, M.J., 2006. The Structural and Hydrothermal Evolution of Intrusion-related Gold Mineralisation at the Brewery Creek Mine. James Cook, Yukon, Canada (348 pp.).
Lindsay, M., Aitken, A.R., Dentith, M.C., Hollis, J.A., Tyler, I.M., 2015a. Mineral Prospectivity of the King Leopold Orogen and Lennard Shelf: Potential Field Analysis in the West Kimberley, Report xx. Geological Survey of Western Australia, Perth.
Lindsay, M., Occhipinti, S.A., Hollis, J.A., Aitken, A., Metelka, V., Dentith, M., Miller, J., Tyler, I.M., 2015b. A Geophysical Investigation of the East Kimberley, Northern Western Australia, Report xx. Geological Survey of Western Australia, Perth.
Lindsay, M., Aitken, A., Ford, A., Dentith, M., Hollis, J., Tyler, I., 2015c. Reducing subjectivity in multi-commodity mineral prospectivity analyses: Modelling the west Kimberley, Australia. Ore Geol. Rev. http://dx.doi.org/10.1016/j.oregeorev.2015.03.022.
London, 2011. Rare earth elements. In: G.S.o. London (Ed.), Geological Society of London. The Geological Society of London.
Loucks, R.R., 2014. Distinctive composition of copper-ore-forming arc magmas. Aust. J. Earth Sci. 61, 5–16.
Luguet, A., Jaques, A.L., Pearson, D.G., Smith, C.B., Bulanova, G.P., Roffey, S.I., Rayner, M.J., Lorand, J.-P., 2009. An integrated petrological, geochemical and Re–Os isotope study of peridotite xenoliths from the Argyle lamproite, Western Australia and implications for cratonic diamond occurrences. Lithos 112S, 1096–1108.
McCuaig, C.T., Hronsky, J.M.A., 2014. The mineral system concept: the key to exploration targeting. Soc. Econ. Geol. 153–175.
McCuaig, C.T., Beresford, S., Hronsky, J.M.A., 2010. Translating the mineral systems approach into an effective exploration targeting system. Ore Geol. Rev. 38, 128–138.
Miller, J.M., Nelson, E.P., Hitzman, M., Muccilli, P., Hall, W.D.M., 2007. Orthorhombic fault-fracture patterns and non-plane strain in synthetic transfer zone during riftng: Lennard shelf, Canning basin, Western Australia. J. Struct. Geol. 29, 1002–1021.
O'Driscoll, E.S.T., 1981. Structural corridors in Landsat lineament interpretation. Mineral. Deposita 16, 85–101.
Page, R.W., Sun, S.-S., 1994. Evolution of the Kimberley Region, W.A. and adjacent Proterozoic inliers — new geochronological constraints. Geological Society of Australia Abstracts, pp. 332–333.
Page, R.W., Griffin, T.J., Tyler, I.M., Sheppard, S., 2001. Geochronological constraints on tectonic models for Australian Palaeoproterozoic high K-granites. J. Geol. Soc. Lond. 158, 535–545.
Rugless, C., Pirajno, F., 1996. Geology and geochemistry of the Copperhead Albitite 'Carbonatite' Complex, East Kimberley, Western Australia. Aust. J. Earth Sci. 43, 311–322.
Sanders, T., 1999. Mineralization of the Halls Creek Orogen, east Kimberley region. Western Australia, Report. West Australia Geological Survey, p. 66 (44 pp.).
Seat, Z., Beresford, S.W., Grguric, B.A., Waugh, R.S., Hronsky, J.M.A., Gee, M., Groves, D.I., Mathison, C.I., 2007. Architecture and emplacement of the Nebo-Babel gabbronorite-hosted magmatic Ni–Cu-PGE sulphide deposit, West Musgrave, Westerna Australia. Mineral. Deposita 42, 551–581.
Sewell, D., 1999. The Koongie Park and Little Mount Isa zinc–copper–lead deposits East Kimberley Region. In: Ferguson, K. (Ed.), Lead, Zinc, and Silver Deposits of Western Australia. Western Australia Geological Survey, pp. 139–155.
Shaw, R., Macias, L.F., 2000. Geophysical expression of the Mafic–ultramafic intrusions and implications for exploration. In: Hoatson, D.M. (Ed.), Geology and Economic Potential of the Palaeoproterozoic Layered Mafic–Ultramafic Intrusions in the East Kimberley, Western Australia. Australian Geological Survey Organisation, Canberra, pp. 173–188.
Shaw, R.D., Meixner, A., Murray, A., 2000. Regional geophysical setting and tectonic implications of the mafic–ultramafic intrusions. In: Hoatson, D.M., Blake, D.H. (Eds.), Western Australia, Volume Bullentin 246. Australian Geological Survey Organisation, Canberra.
Sheppard, S., Griffin, T.J., Tyler, I.M., 1997. Compilation of whole-rock geochemical data for the King Leopold and Halls Creek Orogens. Geological Survey of Western Australia, 1997/4 (138 pp.).
Sheppard, S., Tyler, I.M., Griffin, T.J., Taylor, W.R., 1999. Palaeoproterozoic subduction-related and passive margin basalts in the Halls Creek Orogen, northwest Australia. Aust. J. Earth Sci. 46, 679–690.
Sheppard, S., Griffin, T.J., Tyler, I.M., Page, R.W., 2001. High- and low-K granites and adakites at a Palaeoprtoerozoic plate boundary in northwestern Australia. J. Geol. Soc. Lond. 158, 547–560.
Sheppard, S., Page, R.W., Griffin, T.J., Rasmussen, B., Fletcher, I.R., Tyler, I.M., Kirkland, C.L., Wingate, M.T.D., Hollis, J.A., Thorne, A.M., 2012. Geochronological and isotopic constraints on the tectonic setting of the c. 1800 Ma Hart Dolerite and the Kimberley and Speewah Basins, Northwestern Australia (28 pp.).
Sillitoe, R.H., 2008. Special paper: major gold deposits and belts of the North and South American cordillera: distribution, tectonomagmatic settings, and metallogenic considerations. Econ. Geol. 103 (4), 663–687.
Smithies, R.H., Howard, H.M., Evins, P.M., Kirkland, C.L., Kelsey, D.E., Hand, M., Wingate, M.T.D., Collins, A.S., Belousova, E., 2011. High-temperature granite magmatism, crust-mantle interaction and the Mesoproterozoic intracontinental evolution of the Mesoproterozoic intracontinental evolution of the Musgrave Province, Central Australia. J. Petrol. 52 (5), 931–958.

Smithies, R.H., Kirkland, C.L., Korhonen, F.J., Aitken, A., Howard, H.M., Maier, W.D., Wingate, M.T.D., Quentin de Gromard, R., Gessner, K., 2015. The Mesoproterozoic thermal evolution of the Musgrave Province in central Australia — plume vs. the geological record. Gondwana Res. 27 (4), 1419–1429.

Spratt, J.E., Jones, A.G., Jackson, V.A., Collins, L., Avdeeva, A., 2007. Lithospheric geometry of the Wopmay orogen from a Slave craton to Bear Province magnetotelluric transect. J. Geophys. Res. 114 (18 pp.).

Spratt, J., Dentith, M., Evans, S., Aitken, A., Lindsay, M., Hollis, J., Tyler, I., Joly, A., Shragge, J., 2014. A Magnetotelluric Survey Across the Kimberley Craton, Northern Western Australia. Geological Survey of Western Australia.

Tomkins, A., Grundy, C., 2009. Upper temperature limits of orogenic gold deposit formation: constraints from the granulite-golded Griffin's find deposit, Yilgarn Craton. Econ. Geol. 104, 669–685.

Tomkins, A.G., Weinberg, R.F., McFarlane, C.R.M., 2009. Preferential magma extraction from K- and metal-enriched source regions in the crust. Mineral. Deposita 44, 171–181.

Tyler, I.M., Griffin, T.J., 1990. Structural development of the King Leopold Orogen, Kimberley region, Western Australia. J. Struct. Geol. 12 (5-6), 703–714.

Tyler, I.M., Page, R.W., Griffin, T.J., 1999. Depositional age and provenance of the Marboo formation from SHRIMP- U–Pb zircon geochronology: implications for the early Paleoproterozoic tectonic evolution of the Kimberley region, Western Australia. Precambrian Res. 95, 225–243.

Tyler, I.M., Hocking, R.M., Haines, P.W., 2012. Geological evolution of the Kimberley region of Western Australia. Episodes 35 (1), 298–306.

White, S.H., Muir, M.D., 1989. Multiple reactivation of coupled orthogonal fault systems: an example from the Kimberley region in north Western Australia. Geology 17 (7), 618–621.

White, L.T., Morese, M.P., Lister, G.S., 2014. Lithospheric-scale structures in New Guinea and their control on the location of gold and copper deposits. Solid Earth 5, 163–179.

Wyborn, L.A.I., Heinrich, C.A., Jaques, A.I., 1994. Australian Proterozoic mineral systems: essential ingredients and mappable criteria. Australian Institute of Mining and Metallurgy Annual Conference, pp. 109–115.